

Low- x measurements at STAR

Hank Crawford UCB/SSL

- Program goals for low- x
- X of parton interactions inferred from $\pi^0\pi^0$ and π^0h correlations through NLO pQCD
- Experimental investigation of pp and dAu correlations at $x \sim 0.1-0.001$
- Comparison to theory
- DY extension to lower x

Program

Investigate internal structure of proton

Determine nuclear gluon densities at low x
to understand energy densities in RHI collisions

See color force effects in A_N for π^0 vs γ^*

All are sensitive to low- x parton distributions

Note: NLO pQCD based on fragmentation functions and fits to global data in theoretical framework is the tool to understand the dynamics

Pythia is “tuned” to reproduce experimental data – an excellent tool but susceptible to tweekers

Structure Functions

looking inside a nucleon or nucleus w/ leptons (and quarks?)

$$d\sigma/d\Omega = (d\sigma/d\Omega)_{\text{point}} |F(\mathbf{q})|^2 \quad (\text{note-unpolarized})$$

$$(d\sigma/d\Omega)_{\text{point}} = (d\sigma/d\Omega)_{\text{Mott}} = (Z\alpha)^2 E^2 (1 - v^2 \sin^2(\Theta/2)) / 4k^4 \sin^4\Theta/2$$

static charge target

For static target, $F(\mathbf{q})$ = Fourier transform of charge distribution

F2 derived from electromagnetic probes of nuclear targets that recoil and react
– Are the resulting pdfs universal (ie, hold for strong force as well as em)?

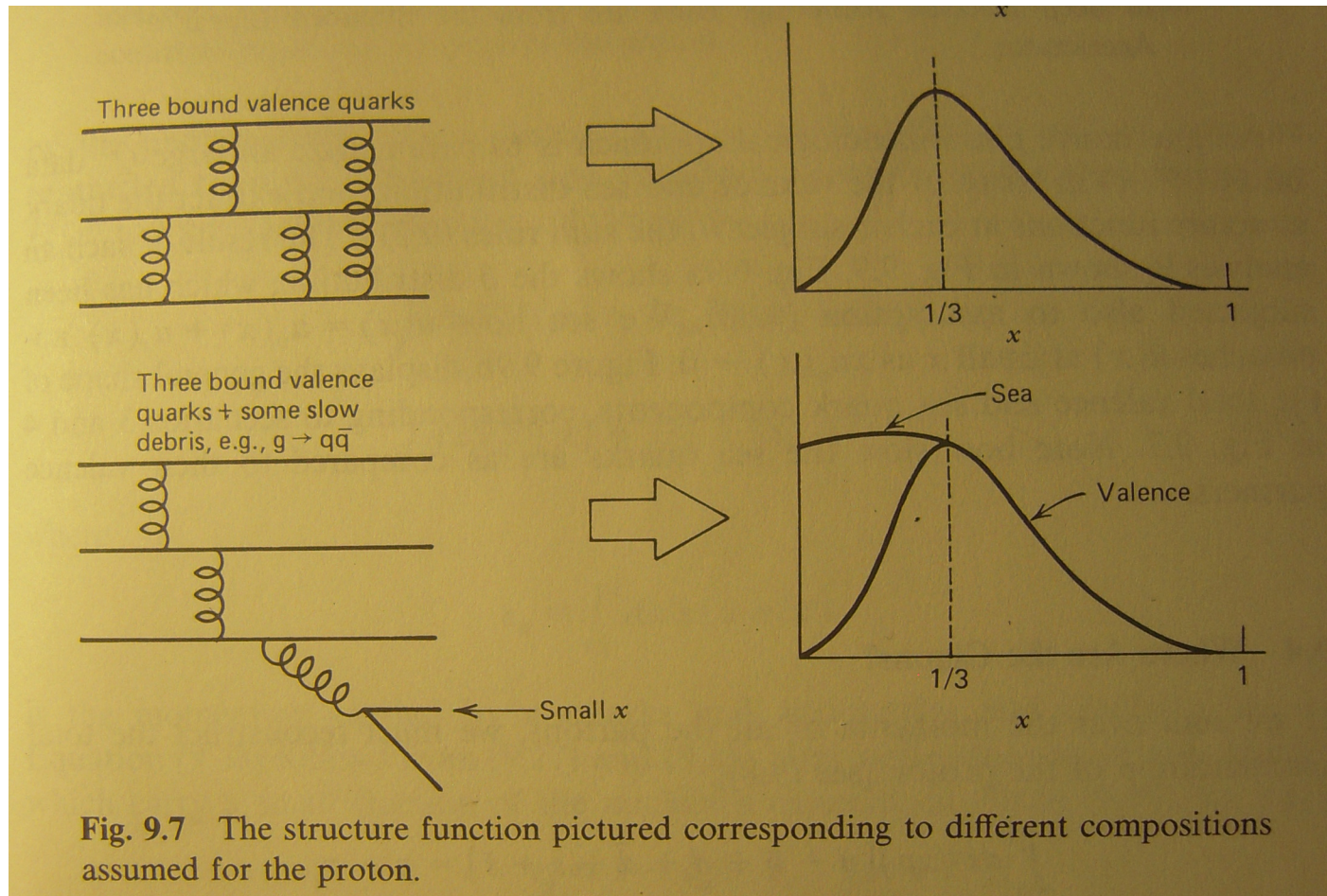
$$2xF_1(x) \approx F_2(x) = x \sum_f e_f^2 f_f(x); \quad x = Q^2/(2Mv); \quad v=(p \cdot q)/M$$

callan-gross $f_f(x)$ is probability to have f-flavor parton with fraction of
protons momentum x

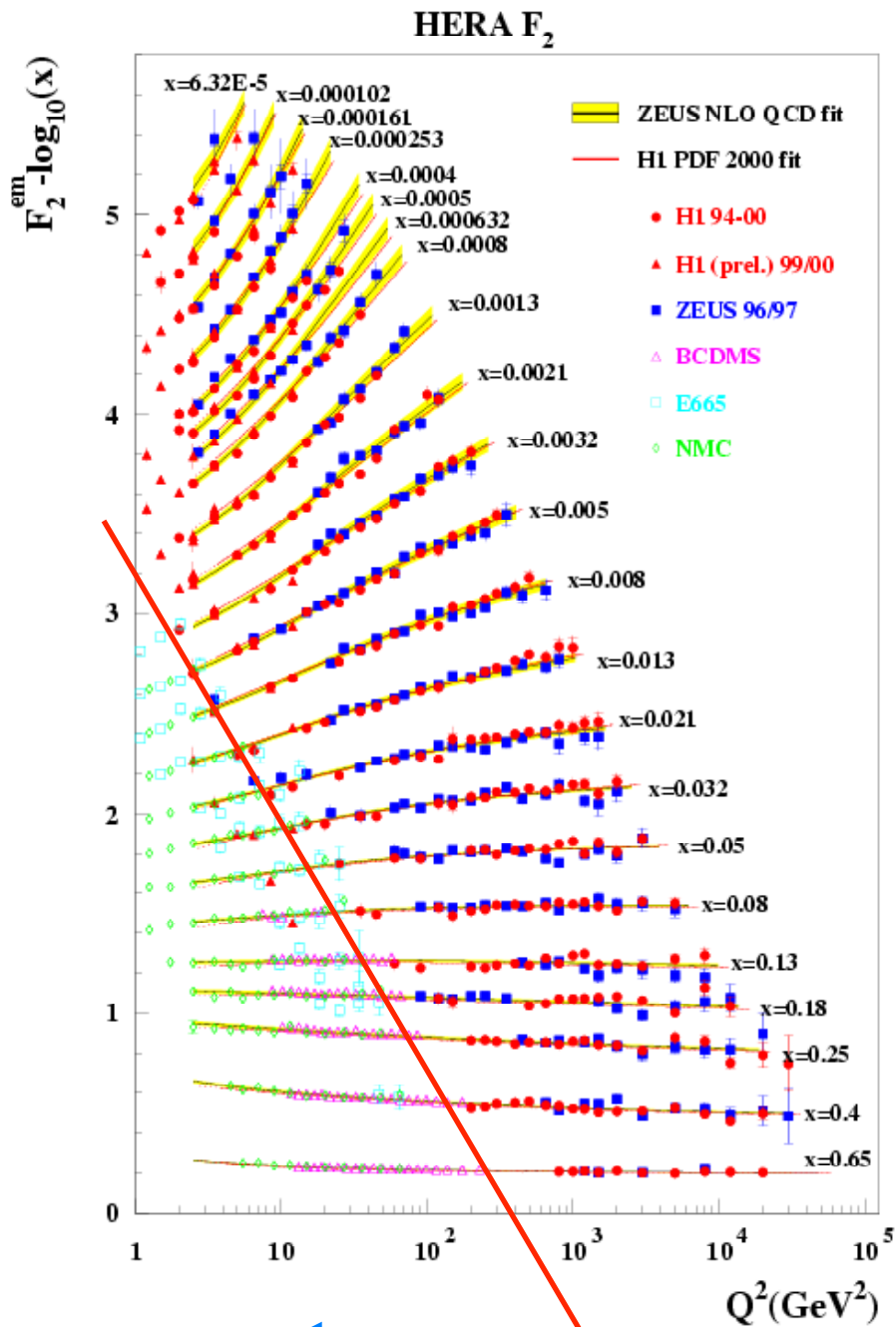
FL = $F_2 - 2xF_1$: gets large at low x

We are interested in what the inside of a proton looks like –
do we start with Thomson's atom?

Pdf – simple



From Halzen and Martin, "Quarks and Leptons", 1984, p201



World Data for (unpolarized) DIS

Note remarkable scaling at $x > 0.1$

Combination of **fixed-target experiments** and results from the HERA collider (DESY) provides a precise determination of the x and Q^2 dependence of the F_2 structure function.

Summary plot from arXiv:hep-ex/0507024, and references therein.

Extracting $g(x)$ from em pdf:
Prytz eqn: $d(F_2)/d(\ln Q^2) \approx g(2x)$

Evolution equations

see Pythia 6.321 Manual

A hard scattering, e.g. in deeply inelastic leptonproduction, will probe the hadron at a given instant. The probe, i.e. the **virtual photon** in the leptonproduction case, is able to resolve fluctuations in the hadron up to the Q^2 scale of the hard scattering. Thus probes at different Q^2 values will seem to see different parton compositions in the hadron. The change in parton composition with $t = \ln(Q^2/\Lambda^2)$ is given by the evolution equations

$$\frac{df_b(x, t)}{dt} = \sum_{a,c} \int \frac{dx'}{x'} f_a(x', t) \frac{\alpha_{abc}}{2\pi} P_{a \rightarrow bc} \left(\frac{x}{x'} \right) . \quad (187)$$

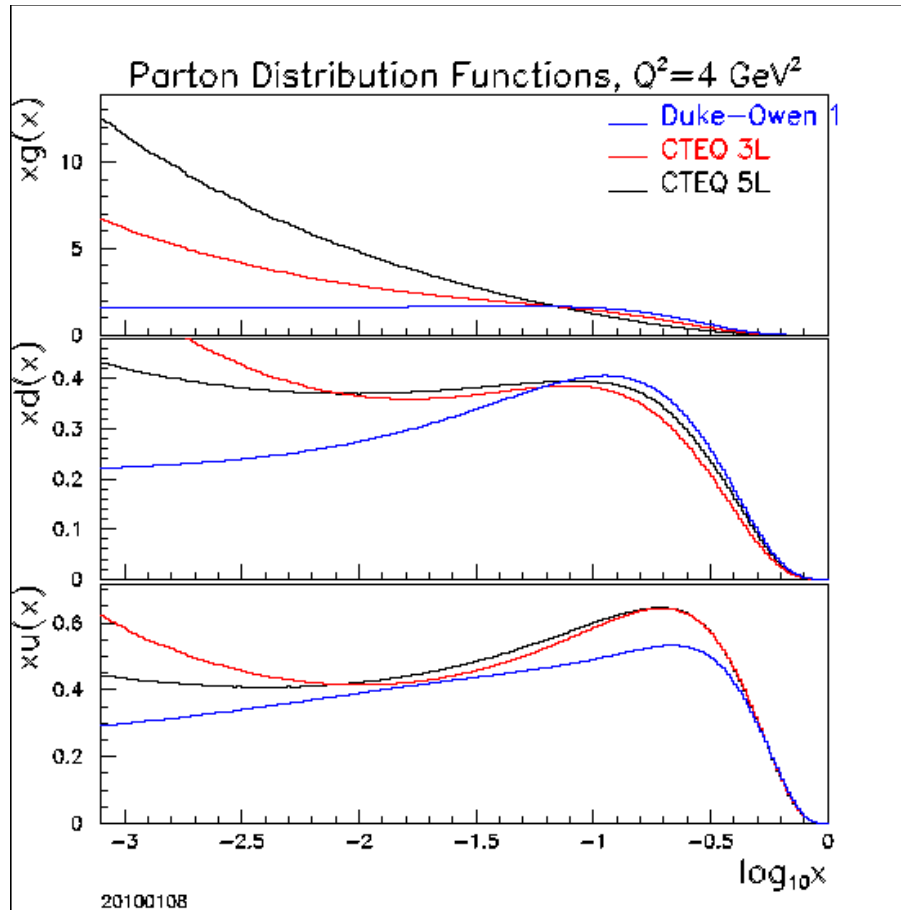
Here the $f_i(x, t)$ are the parton-distribution functions, expressing the probability of finding a parton i carrying a fraction x of the total momentum if the hadron is probed at virtuality Q^2 . The $P_{a \rightarrow bc}(z)$ are given in eq. (164). As before, α_{abc} is α_s for QCD shower and α_{em} for QED ones.

The splitting kernels $P_{a \rightarrow bc}(z)$ are

$$\begin{aligned} P_{q \rightarrow qg}(z) &= C_F \frac{1+z^2}{1-z} , \\ P_{g \rightarrow gg}(z) &= N_C \frac{(1-z(1-z))^2}{z(1-z)} , \\ P_{g \rightarrow q\bar{q}}(z) &= T_R (z^2 + (1-z)^2) , \\ P_{q \rightarrow q\gamma}(z) &= e_q^2 \frac{1+z^2}{1-z} , \\ P_{\ell \rightarrow \ell\gamma}(z) &= e_\ell^2 \frac{1+z^2}{1-z} , \end{aligned} \quad (164)$$

with $C_F = 4/3$, $N_C = 3$, $T_R = n_f/2$ (i.e. T_R receives a contribution of 1/2 for each allowed $q\bar{q}$ flavour), and e_q^2 and e_ℓ^2 the squared electric charge (4/9 for u-type quarks, 1/9 for d-type ones, and 1 for leptons).

PDFs before and after HERA



At RHIC $Q^2 \sim p_T^2$
Our $p_T \sim 2 \text{ GeV}$
Is sensitive to
 $0.001 < x < 0.01$

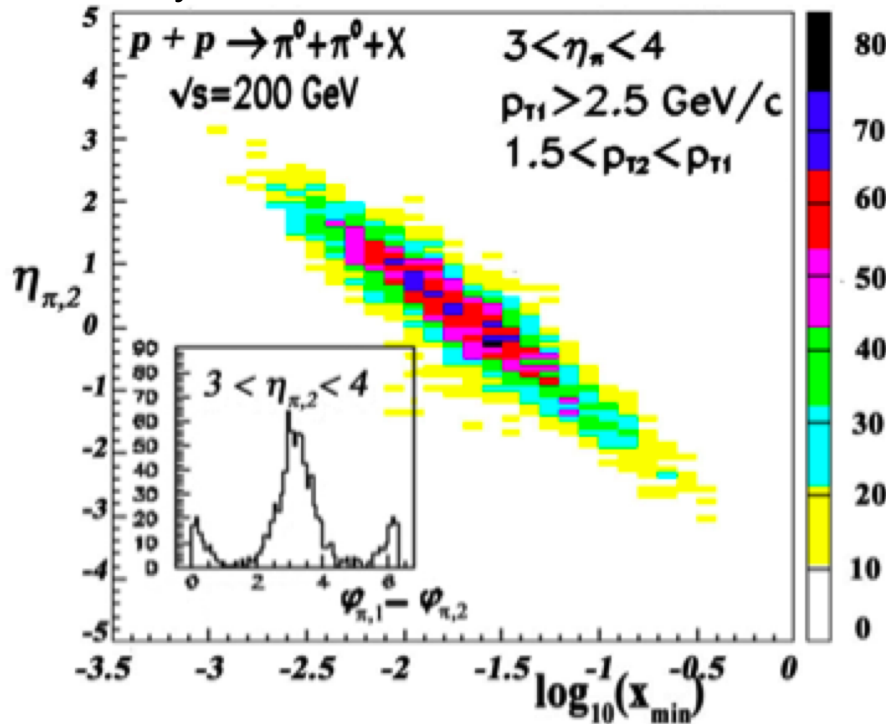
Note the large changes
in $xg(x)$ at low x

in range .01-.001 we
can already contribute

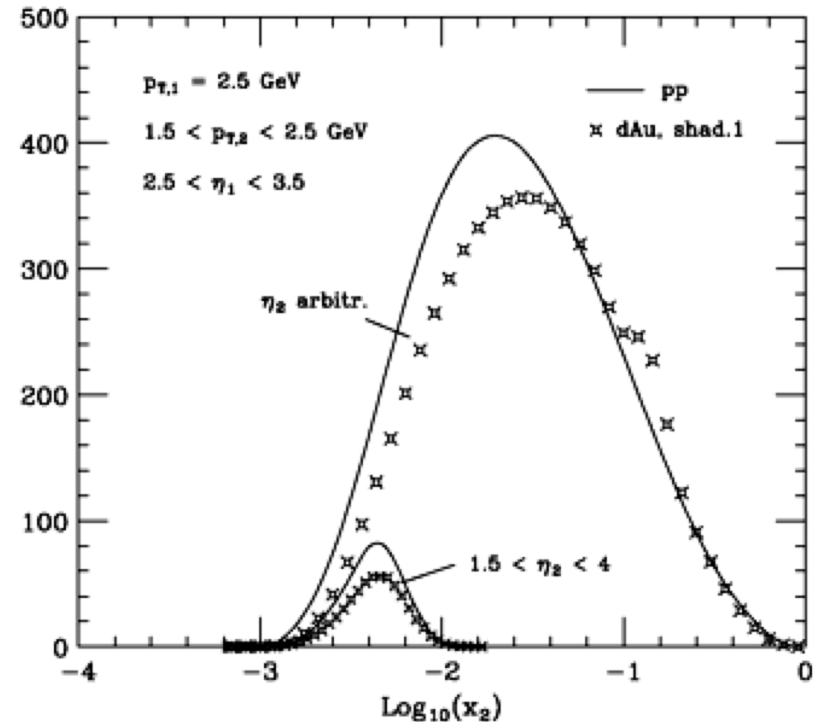
X1 and X2

momentum fractions of interacting partons

Pythia 6.222

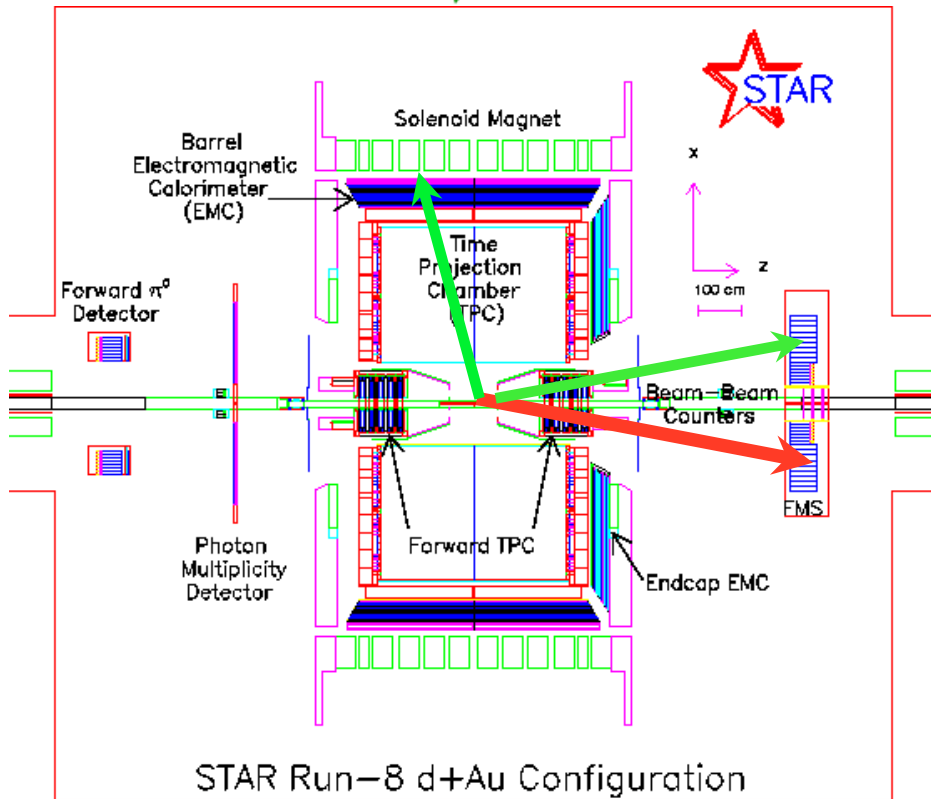
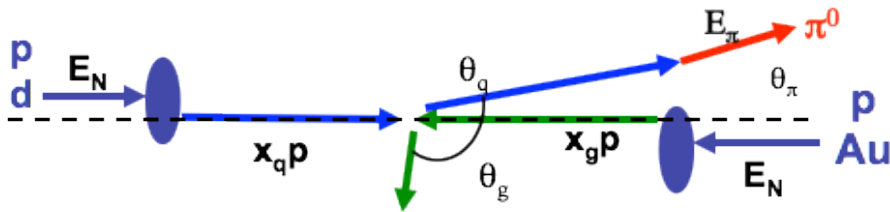


pQCD : GSV PhysLetB 603(2004)173

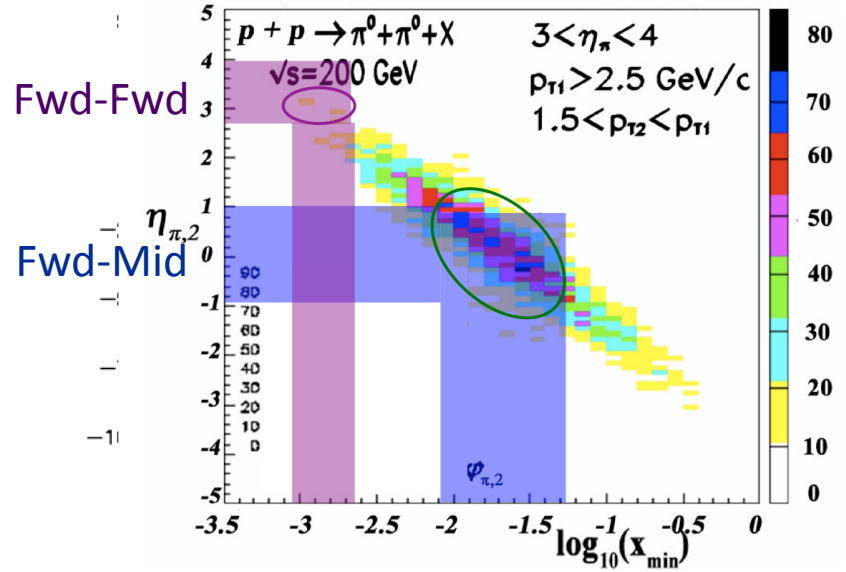
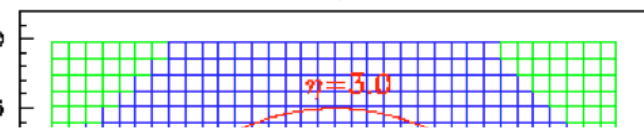


Get x from correlations between a trigger or leading particle (a π^0 in the FMS) and a subleading particle (a TPC track hadron, or a BEMC π^0 , or another FMS π^0)

2-body kinematics at STAR

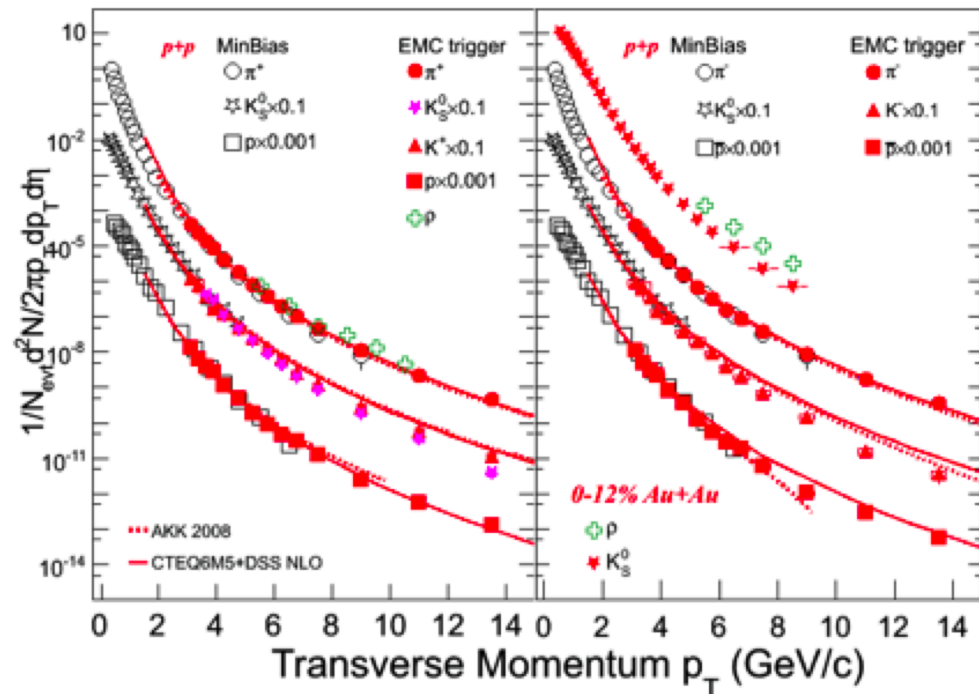
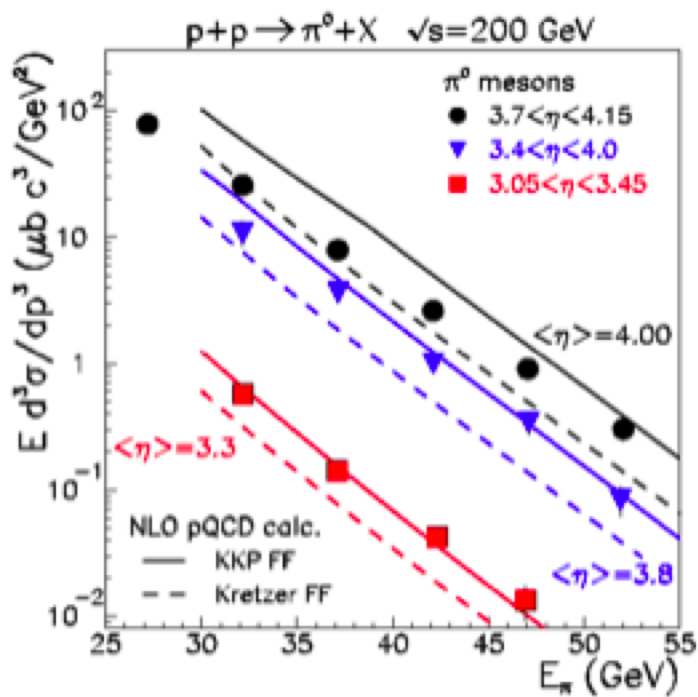


- Forward Meson Spectrometer (FMS)
- trigger π^0
- Time Projection Chamber (TPC)
- associated π^0
- Barrel EM Calorimeter (EMC)
- associated π^0
- FMS
- a



NLO pQCD

Cross sections agree with NLO pQCD down to $p_T \sim 2$ GeV/c over a wide range of pseudorapidity, $0 < \eta < 3.8$, at $\sqrt{s} = 200$ GeV



PRL 97 2006 152302 nucl-ex/0602011

Our π^0 data is used in "Global analysis of fragmentation functions for pions and kaons and their uncertainties", D. de Florian, R. Sassot, M. Stratmann, Phys. Rev. D76 (2007) 114010.

Min bias pp data:
PLB 637 (2006) 161
Hi- p_T data: Xu Y. QM09

Fits to “raw” data

Pythia GSTAR vs Clusters in data

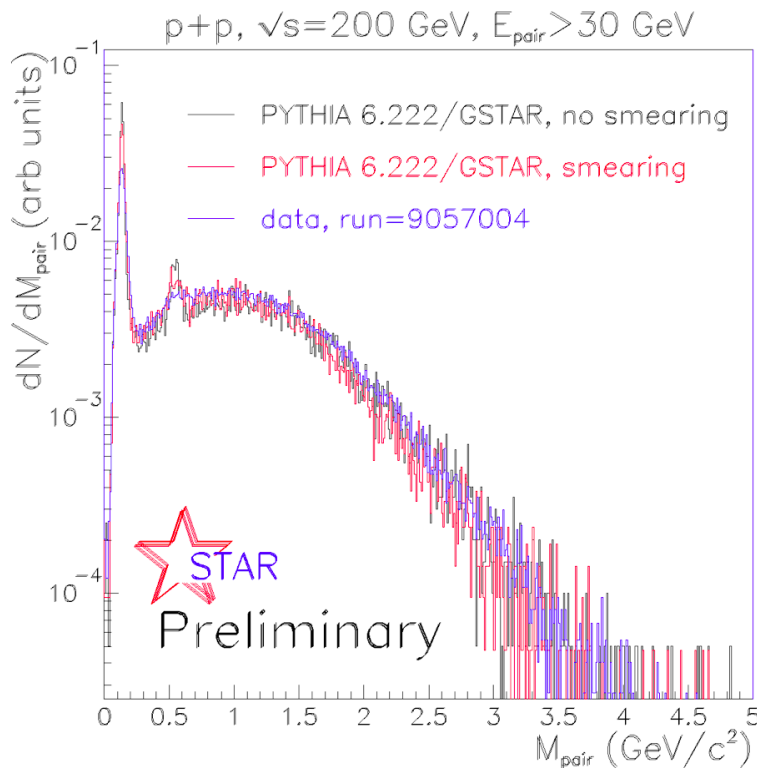
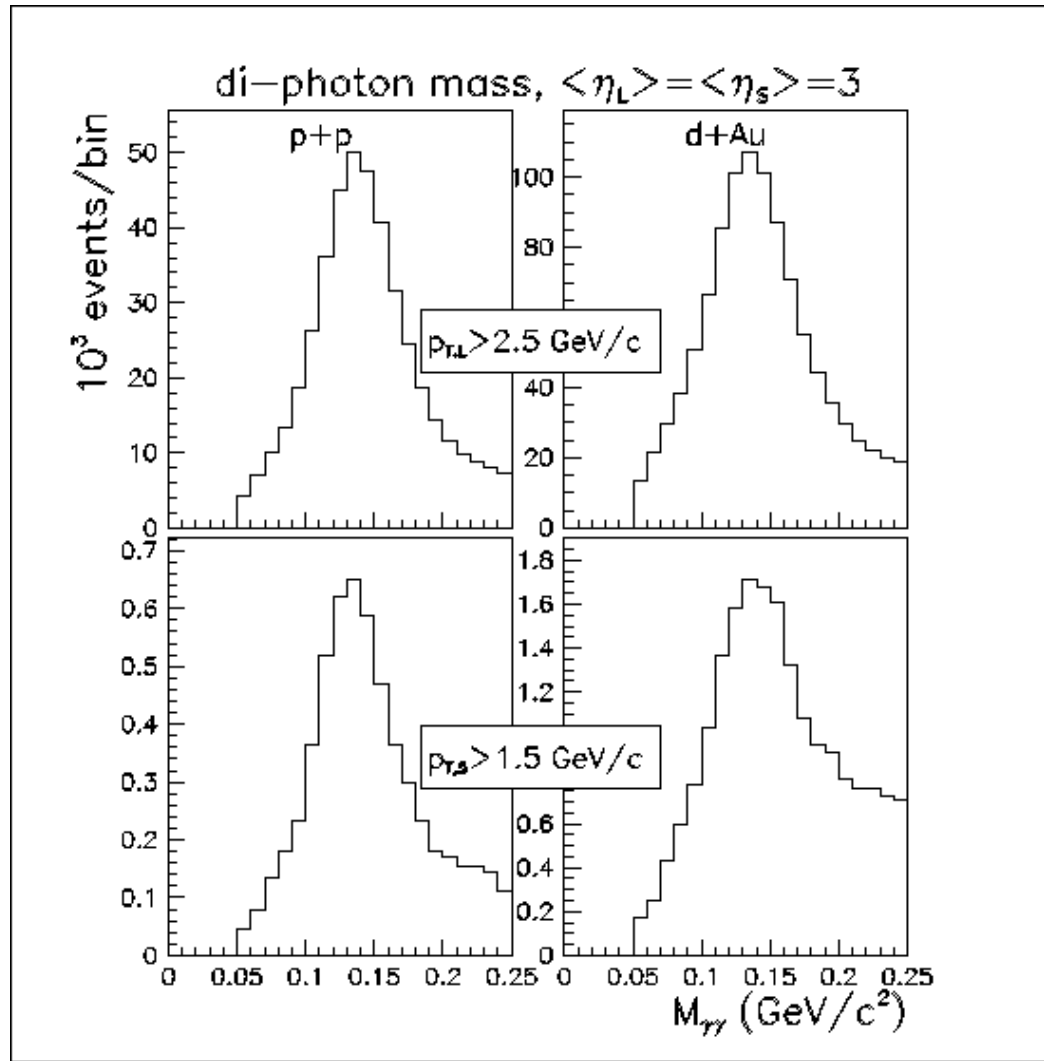


Fig. 4 Intercomparison of cluster pair invariant mass from data (blue) to full PYTHIA/GEANT simulations from the Forward Meson Spectrometer. In general, most aspects of the p+p data are present in the PYTHIA/GEANT reconstructions [8].

arXiv:0906.23332

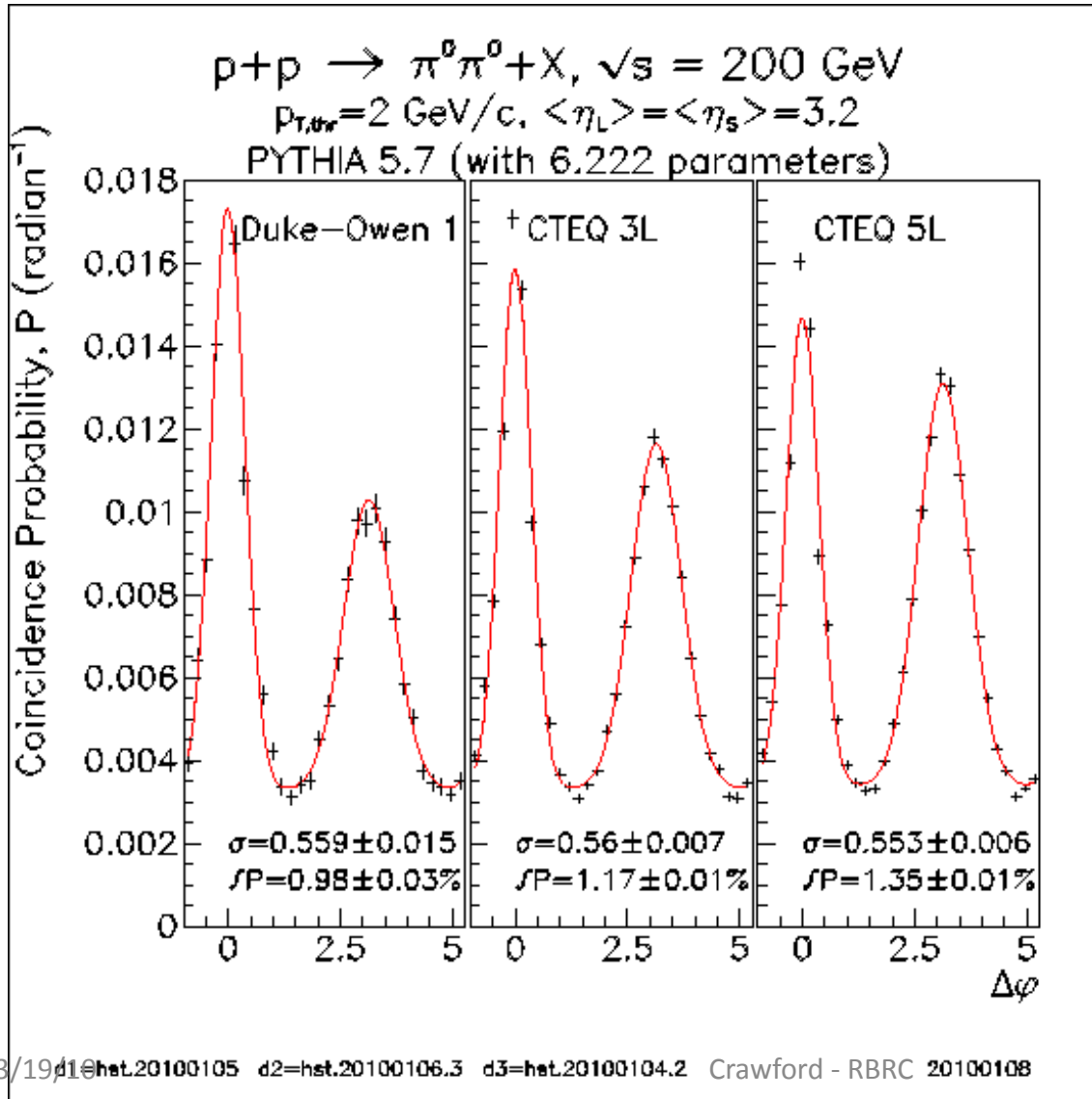
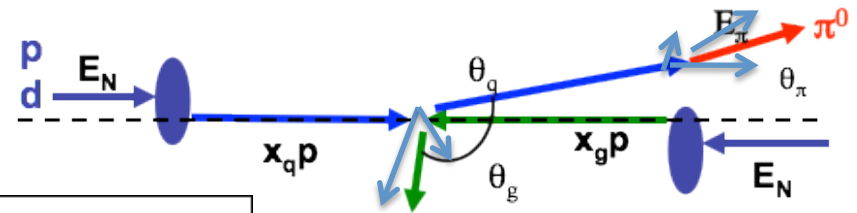
Pythia 6.222 agrees well with our data

General π^0 reconstruction



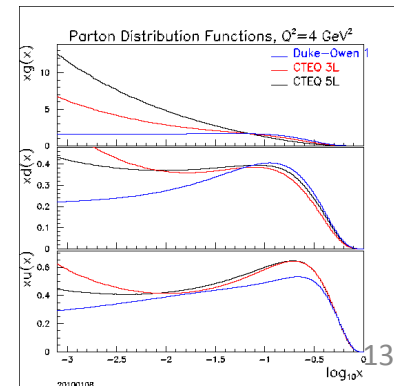
Typical mass
Cuts in analysis
 $0.1 < M_{\gamma\gamma} < 0.2$ are
Identified as π^0

Pythia Pdf sensitivity

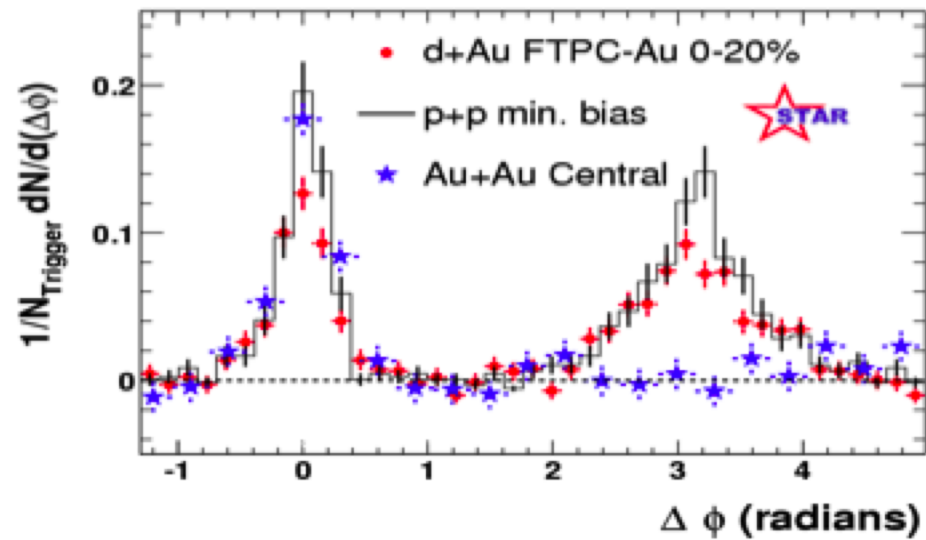


Our signal:
 Same side and
 away side peaks
 and widths

(and composition)

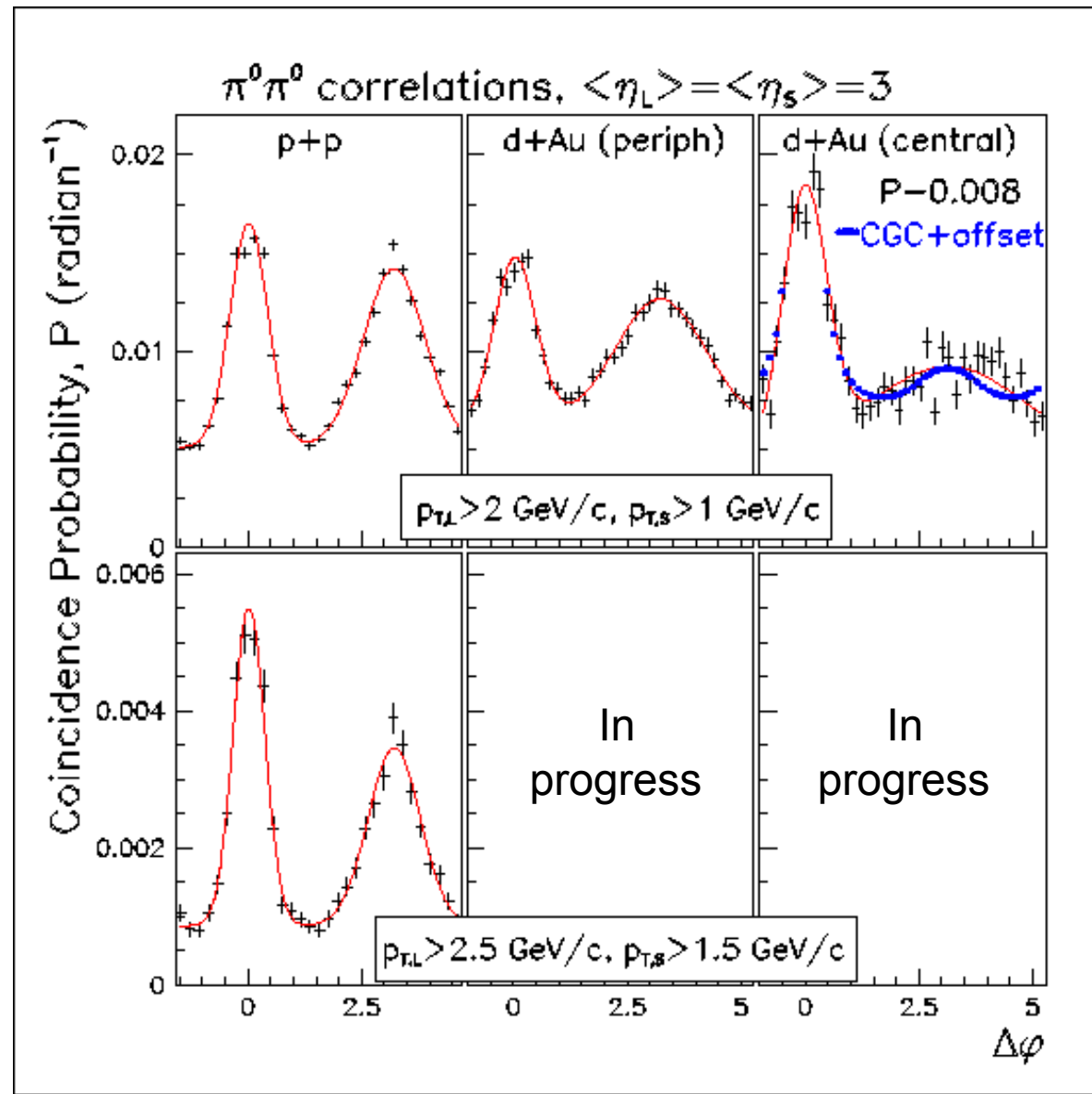


First data – run 3



Away-side peak is gone in central AuAu collisions
Suppression as a function of “b”

FMS-FMS Data



Blue is from
Marquette
See below

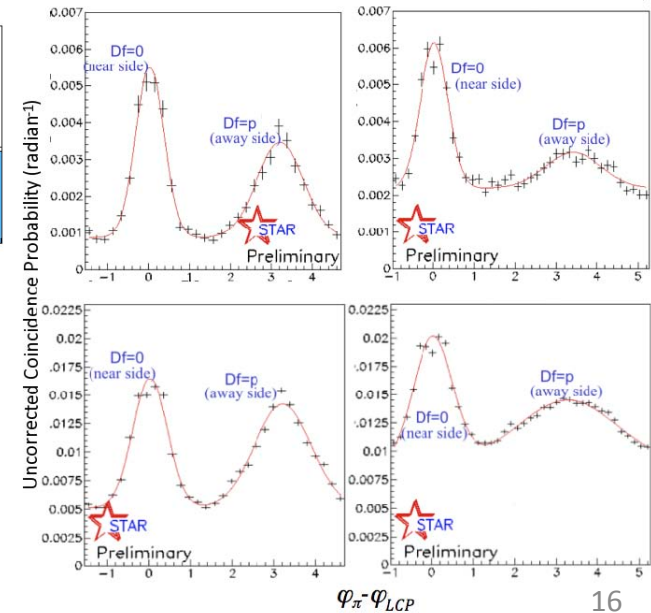
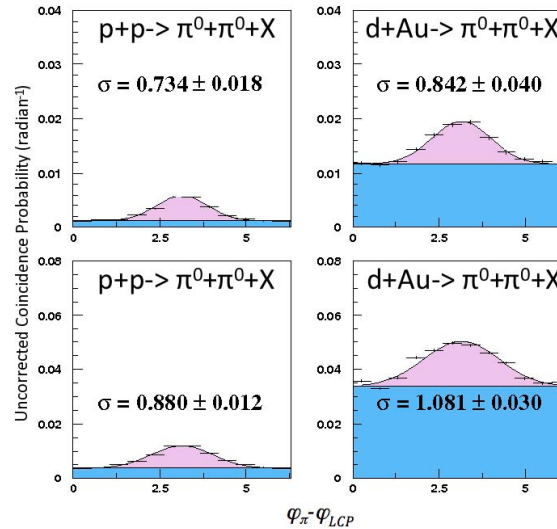
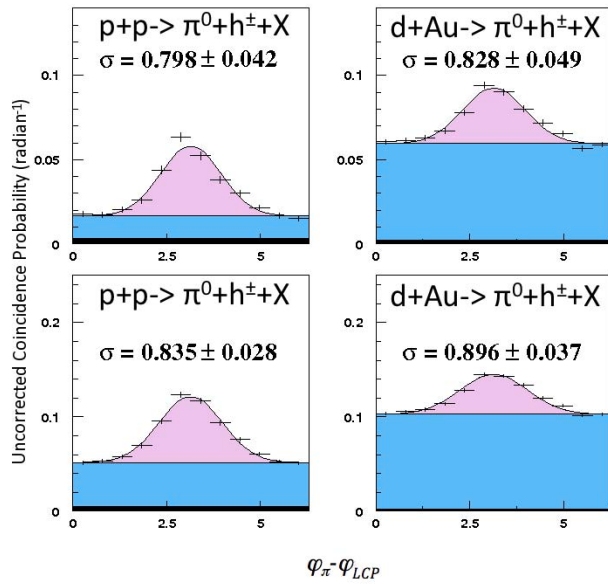
Spanning $-1 < \eta < 4.1$ with FMS trigger

$\pi^0 h$ -mid, $\pi^0 \pi^0$ -mid, $\pi^0 \pi^0$ -fwd

Made possible by STAR coverage

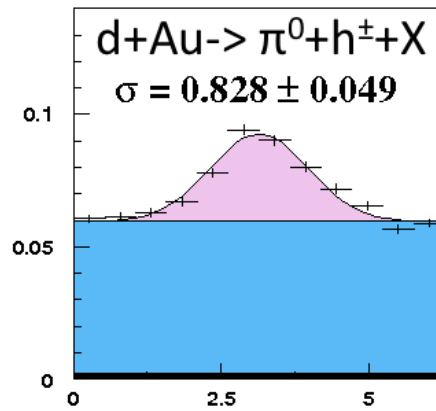
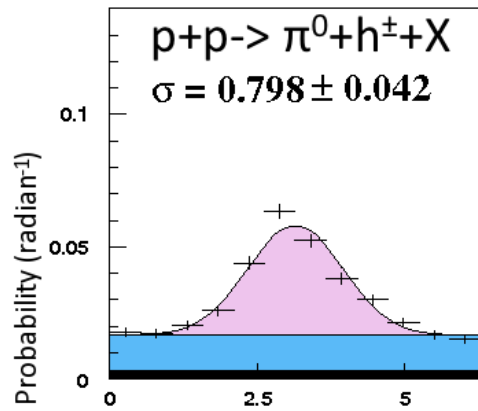
Centrality averaged

2 trigger p_T s each

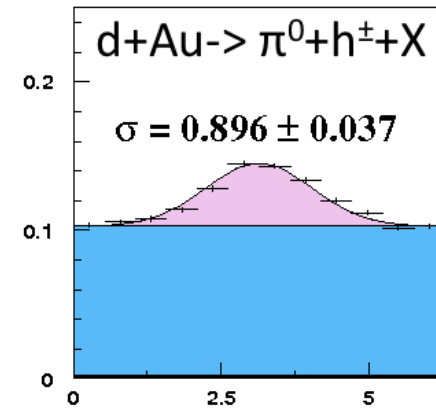
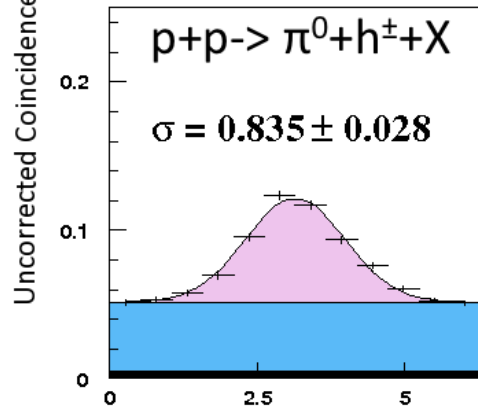


FMS-TPC: $\pi^0_{\text{FWD}}-h_{\text{MID}}$ p_T dependence

$p+p$  STAR PRELIMINARY $d+Au$



$p_T^{(\text{FMS})} > 2.5 \text{ GeV} ; p_T^{(\text{TPC})} > 1.5 \text{ GeV}$



$p_T^{(\text{FMS})} > 2.0 \text{ GeV} ; p_T^{(\text{TPC})} > 1.0 \text{ GeV}$

$\varphi_\pi - \varphi_{LCP}$

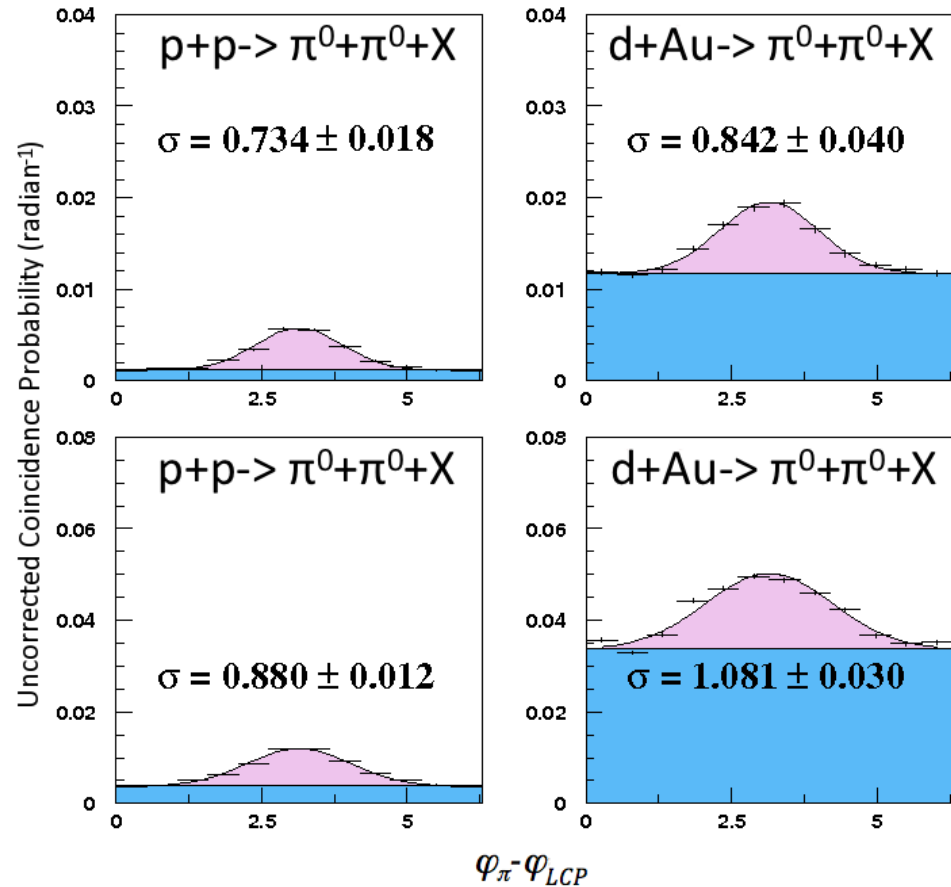
$dAu \approx pp$

FMS-BEMC: $\pi^0_{\text{FWD}}-\pi^0_{\text{MID}}$ p_T dependence

$$p_T^{(\text{FMS})} > 2.5 \text{ GeV} ; p_T^{(\text{bEMC})} > 1.5 \text{ GeV}$$

$$p_T^{(\text{FMS})} > 2.0 \text{ GeV} ; p_T^{(\text{bEMC})} > 1.0 \text{ GeV}$$

Gaussian+constant fit to away-side
dAu significantly broader than pp



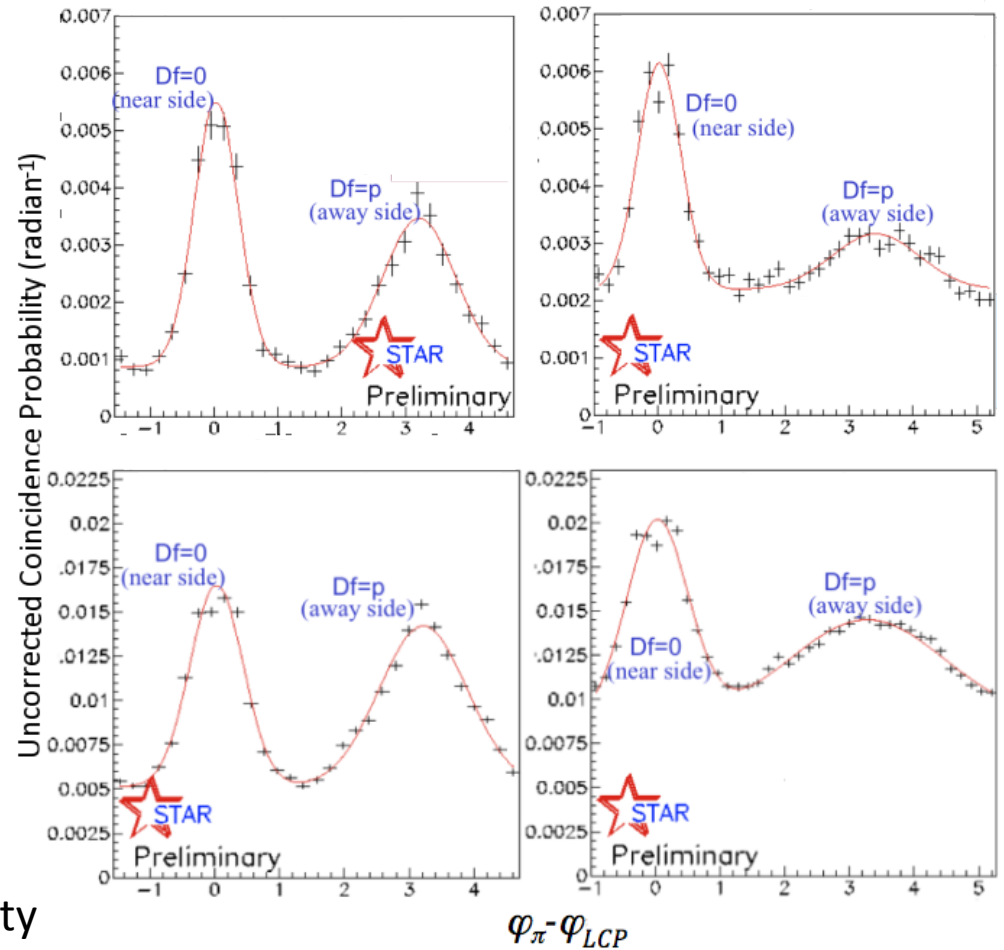
FMS-FMS : π^0 - π^0 p_T dependence

$p_{TL}^{(FMS)} > 2.5 \text{ GeV}; p_{TS}^{(FMS)} > 1.5 \text{ GeV}$

$p_{TL}^{(FMS)} > 2.0 \text{ GeV}; p_{TS}^{(FMS)} > 1.0 \text{ GeV}$

dAu much broader than pp

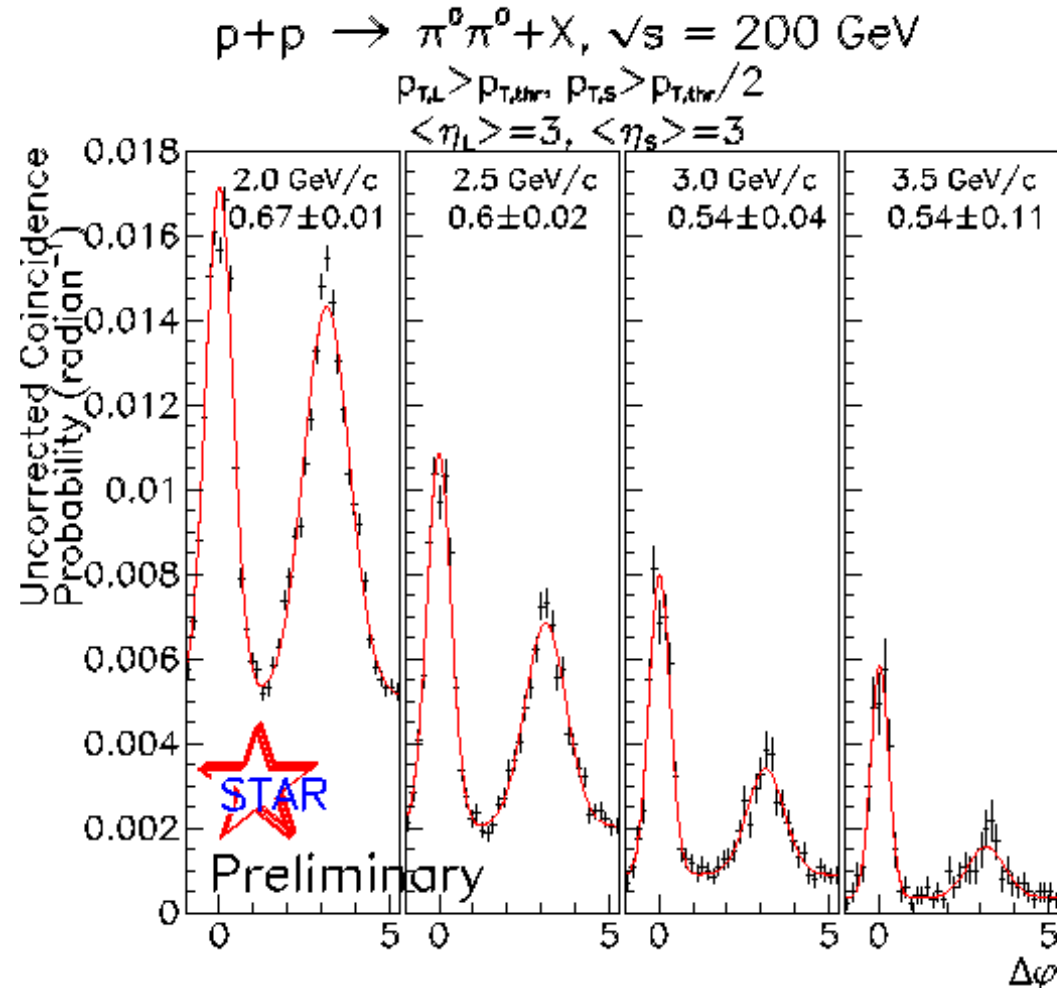
In addition to p_T , we can cut on centrality



Scanning pt

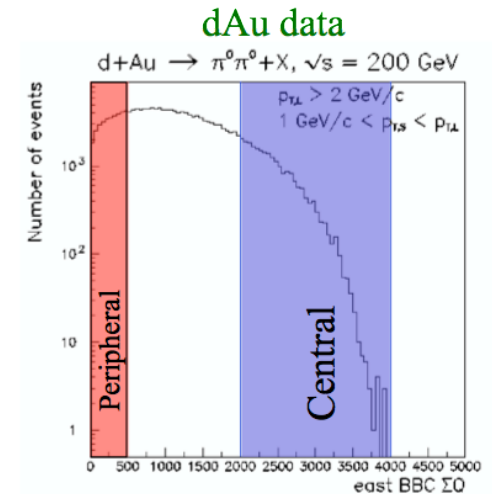
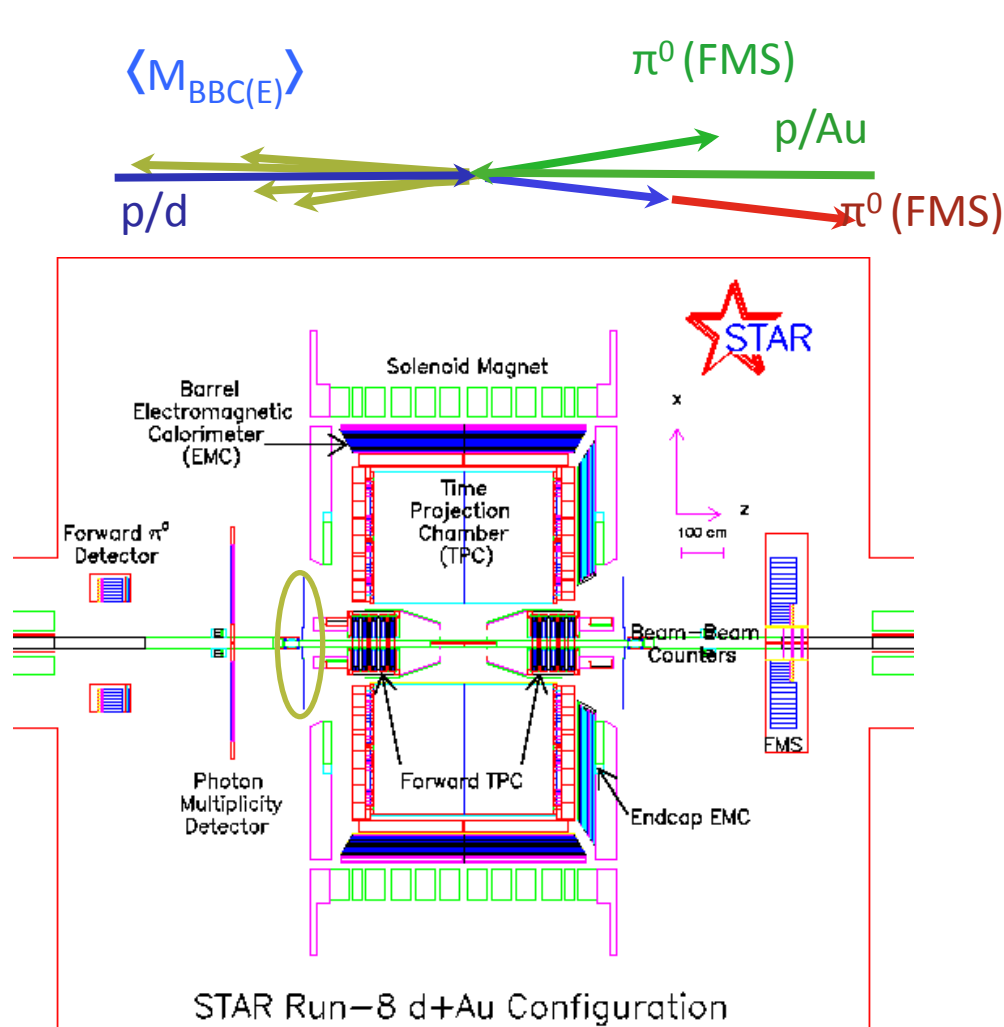
Normalized to number of events with leading $P_T(\pi^0) > 2.0 \text{ GeV}$

No efficiency corrections (may have some ϕ dependence)



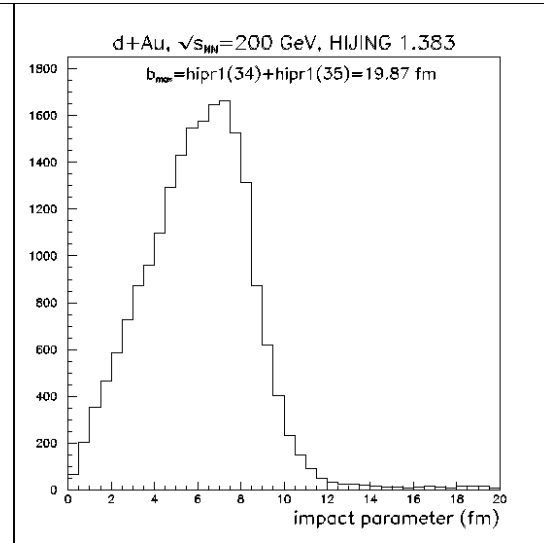
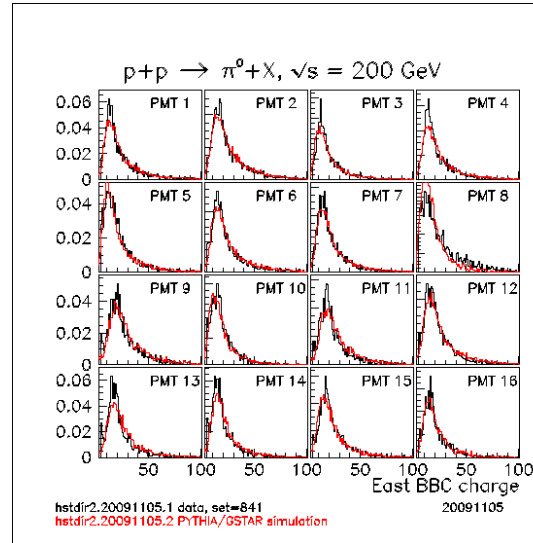
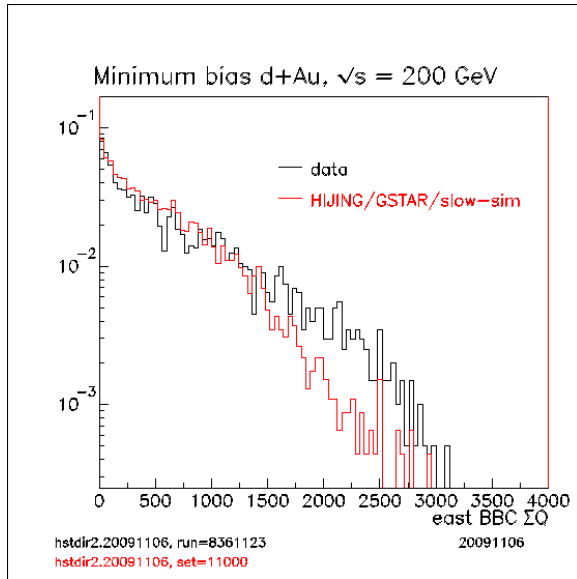
Wider range p_T scan ($p_T^{\text{Trig}} = 2.0$ to 3.5 GeV , $p_T^{\text{Asso}} = p_T^{\text{Trig}} / 2$) for dAu is coming

Centrality dependence of correlations

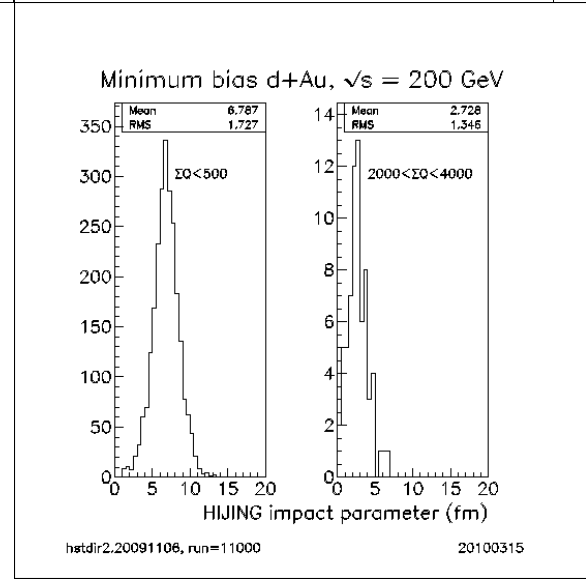


- Saturation expected more when thick part of the nucleus is probed
- Centrality selection through Au-side multiplicity
- Selection: charge sum from east (Au side: $-5.0 < \eta_{BBC} < -3.4$) BBC phototubes

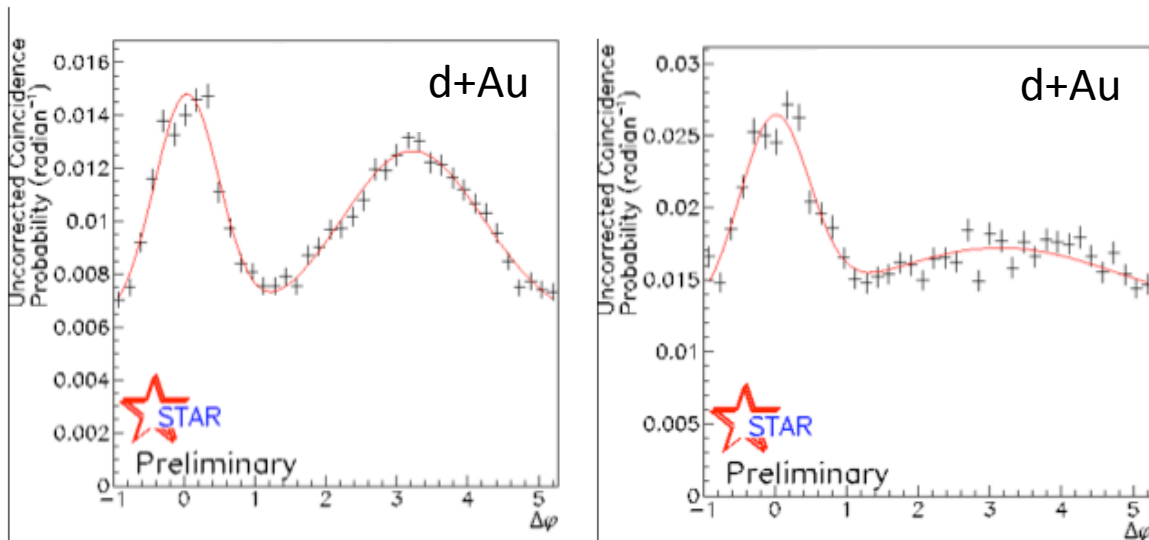
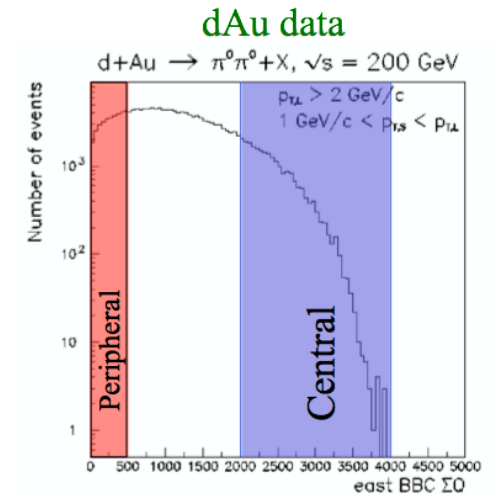
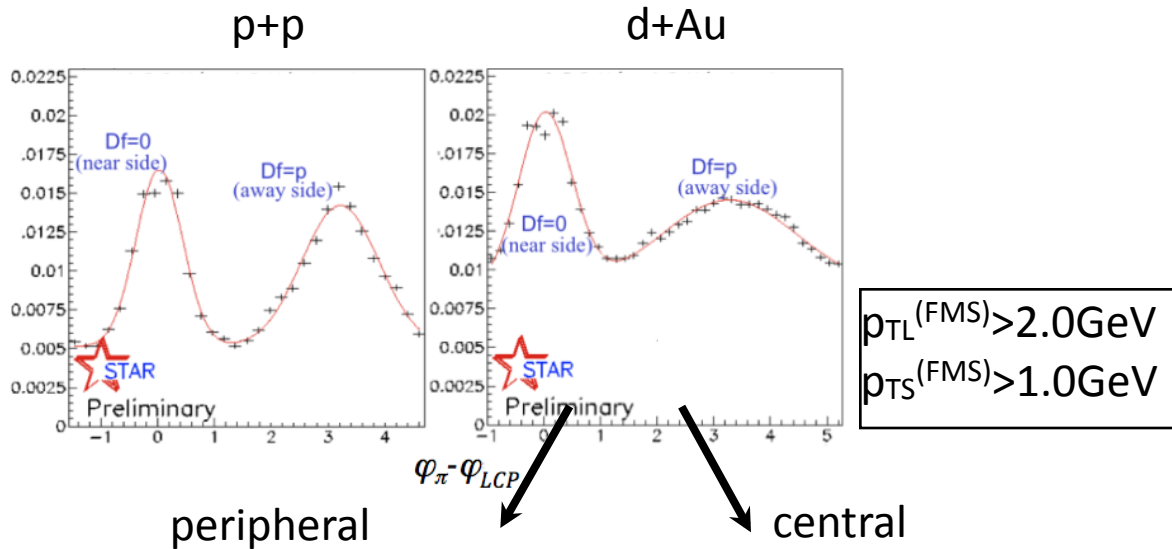
Impact parameter b in Hijing



ΣQ_{BBCE}		$\langle b \rangle$ (fm)	RMS.b (fm)
min	max		
0	500	6.8	1.7
2000	4000	2.7	1.3

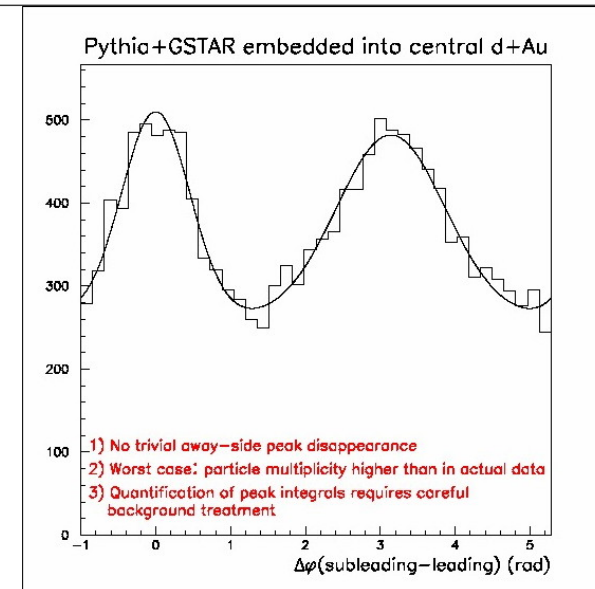
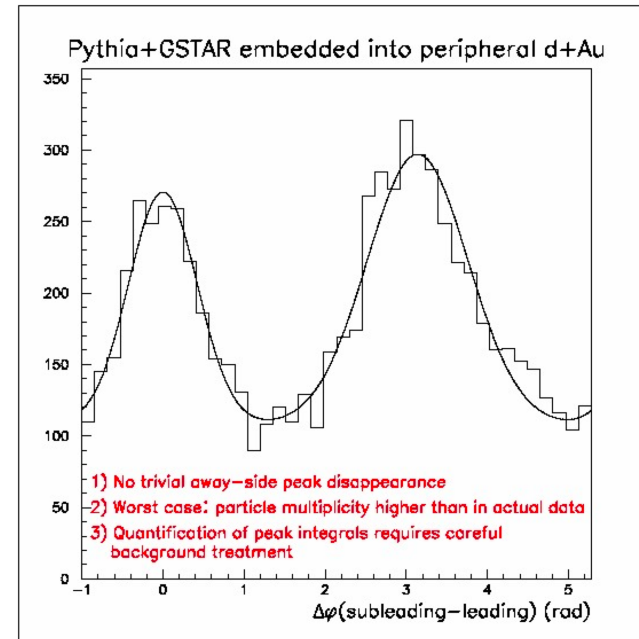
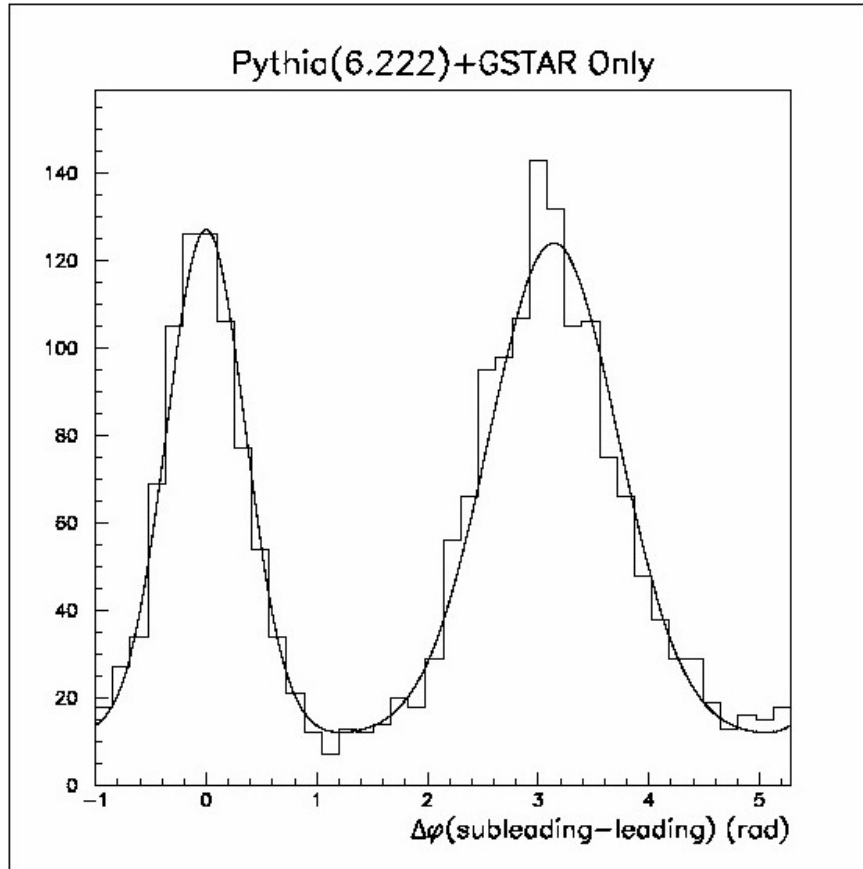


Centrality dependence of correlations



- Near-side peak similar p+p vs. d-Au
- Away-side signal changing with centrality:
 - Peripheral d+Au collisions similar to p+p
 - Central d+Au collision show strong suppression

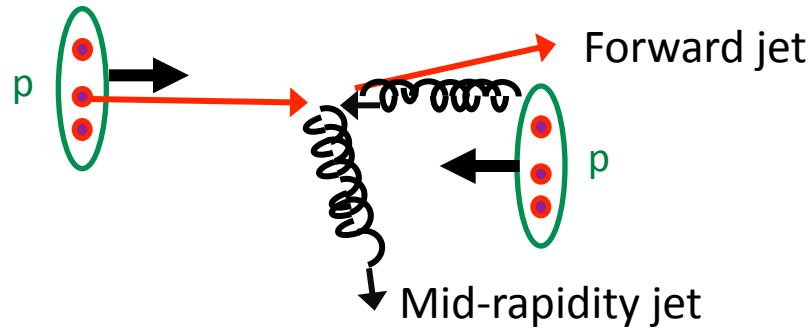
Embedding Study



Correlation preserved even with mean multiplicity from embedding > multiplicity for triggered dAu data

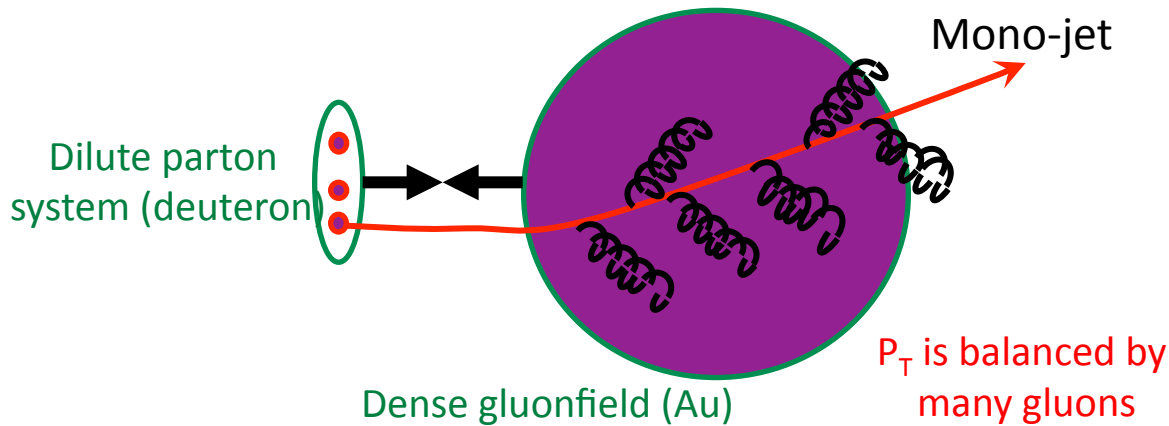
Back-to-back Angular Correlations

pQCD $2 \rightarrow 2$ process = back-to-back di-jet (Works well for p+p)



With high gluon density

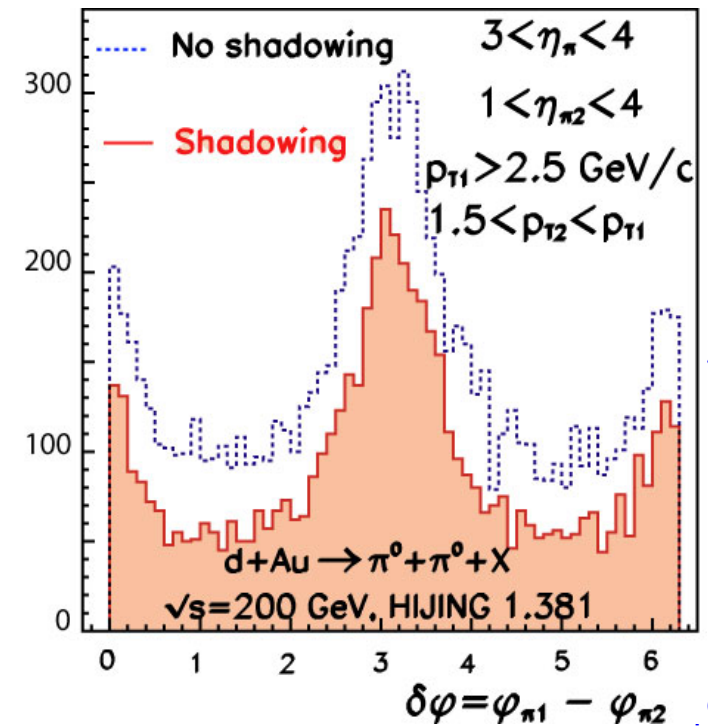
$2 \rightarrow 1$ (or $2 \rightarrow$ many) process = Mono-jet ?



CGC predicts suppression of back-to-back correlation

Conventional shadowing changes yield, but not angular correlation

d+Au in HIJING



Comparison w/ Marquette

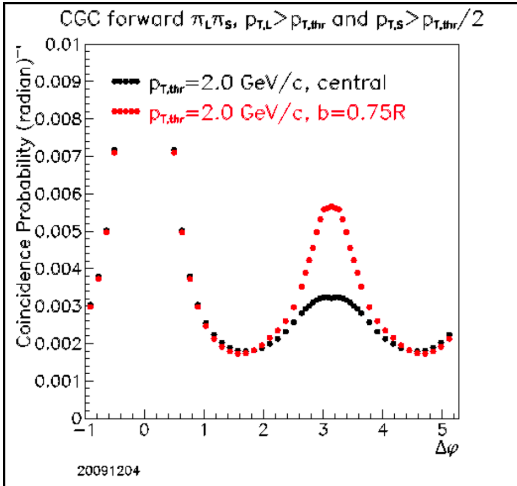


Fig. 2b Theoretical predictions in the framework of [1] for the centrality dependence of azimuthal correlations for d+Au collisions

CGC with $Q_0^2=1.5 \text{ GeV}^2$

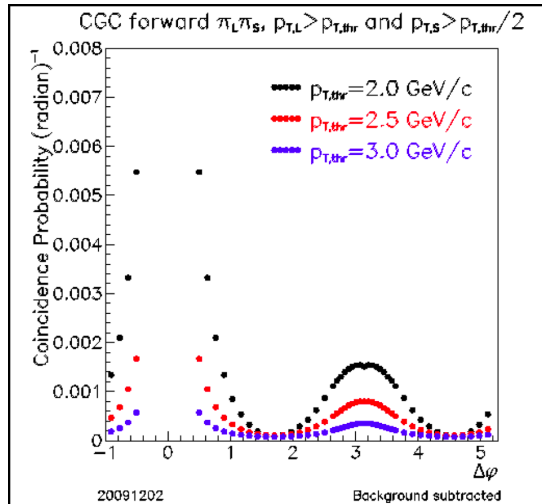
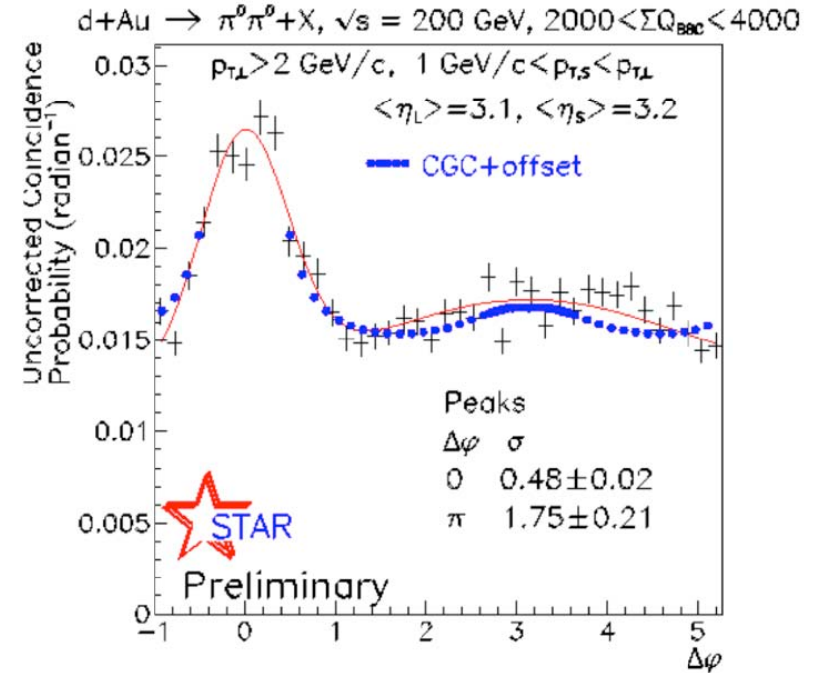


Fig. 2a Theoretical predictions in the framework of [1] for the p_T dependence of azimuthal correlations for central d+Au collisions.



Cyrille Marquet: arXiv:0708.0231
Nucl.Phys.A796:41-60,2007

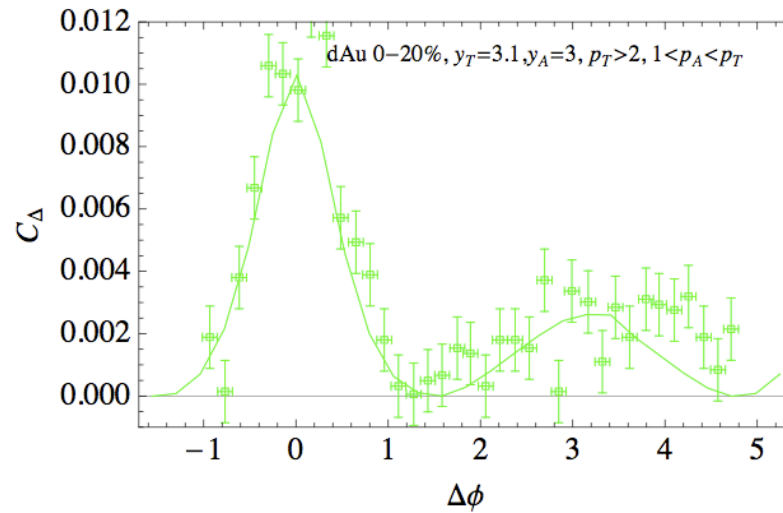
b=0

CM doing b strips
to make better
comparison

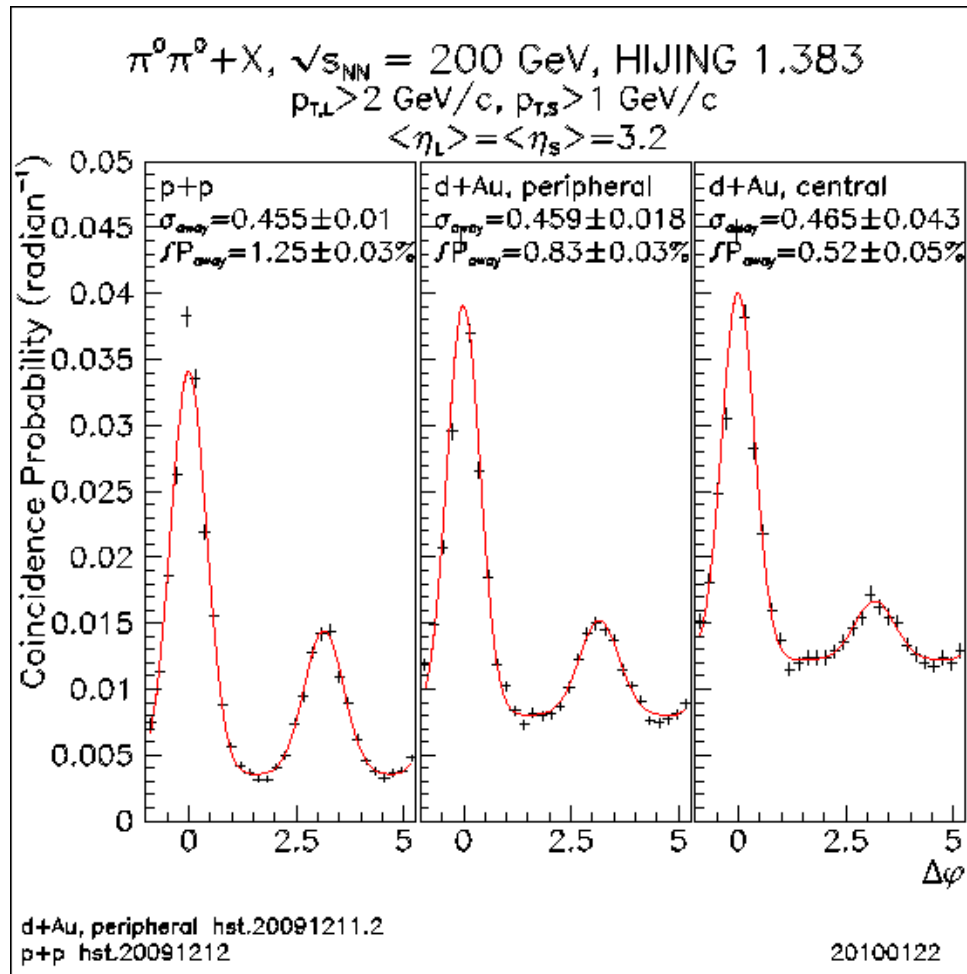
Comparison with Tuchin

Kirill Tuchin: arXiv:0912.5479v1
normalized to peak height

CGC with $Q_0^2 \sim 1.5 \text{ GeV}^2$



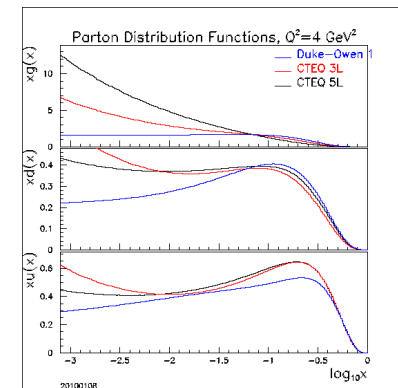
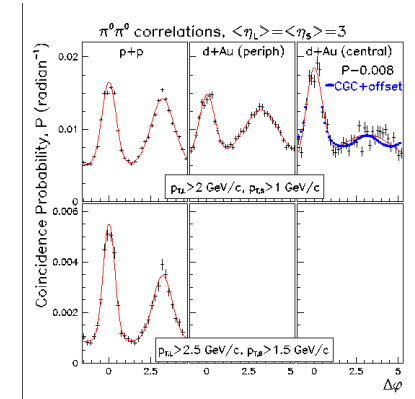
Comparison to Hijing



Does not reproduce data

Uses Duke-Owen
 Which predates
 HERA

Run8 data (see#16)



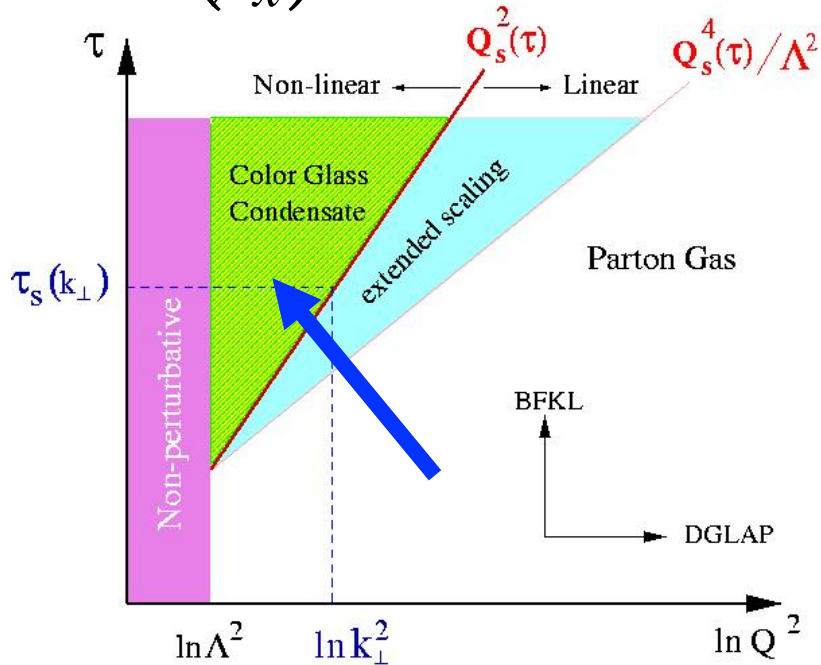
Also have uRQMD

(See#14)

Forward rapidity d+Au

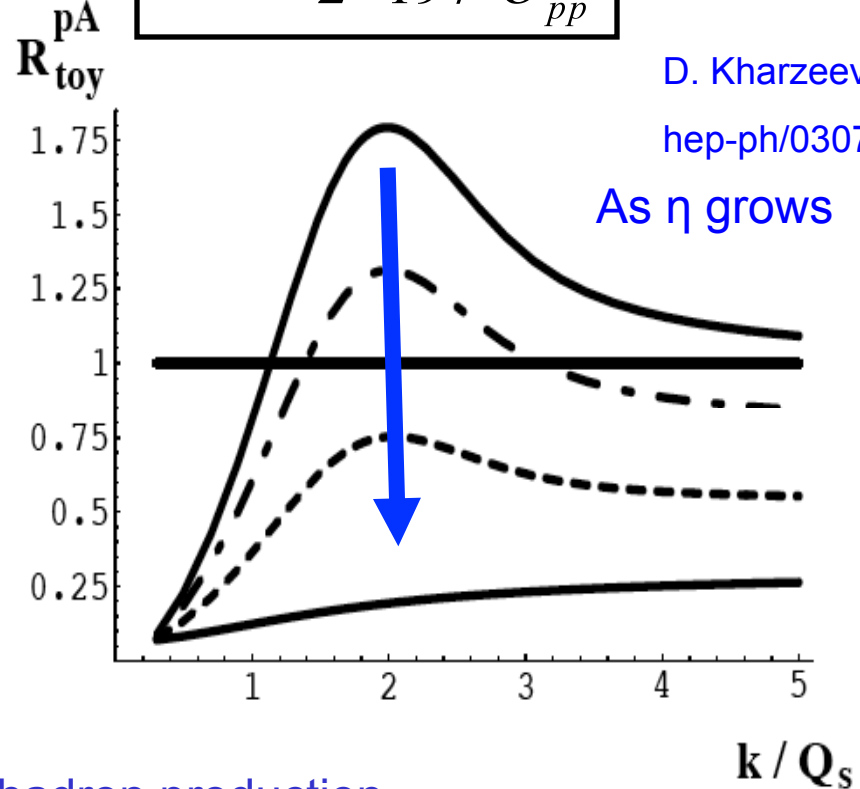
Expectations from Color Glass Condensate

$\tau = \ln(1/x)$ τ related to rapidity of produced hadrons.



Iancu and Venugopalan, hep-ph/0303204

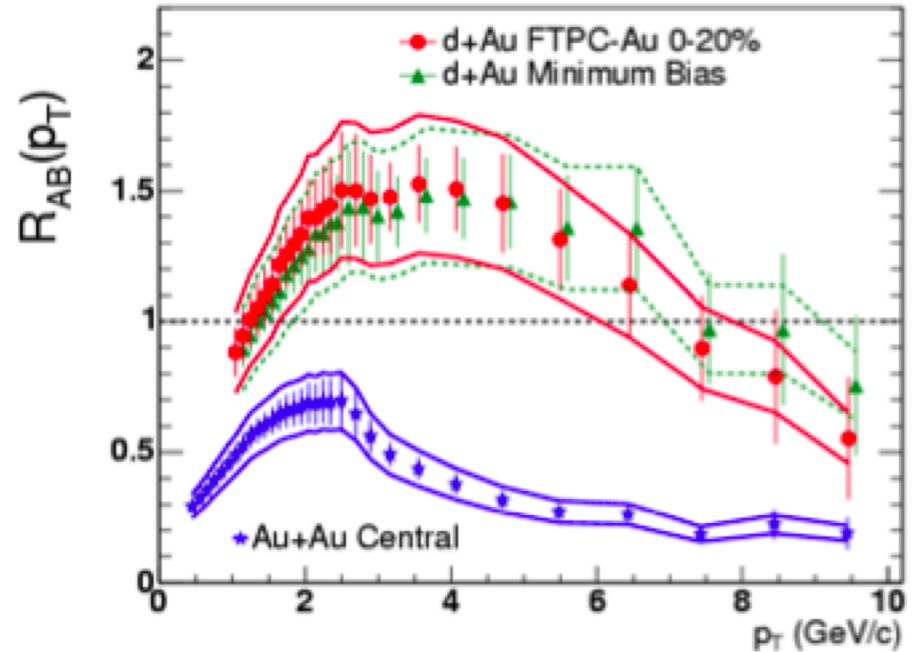
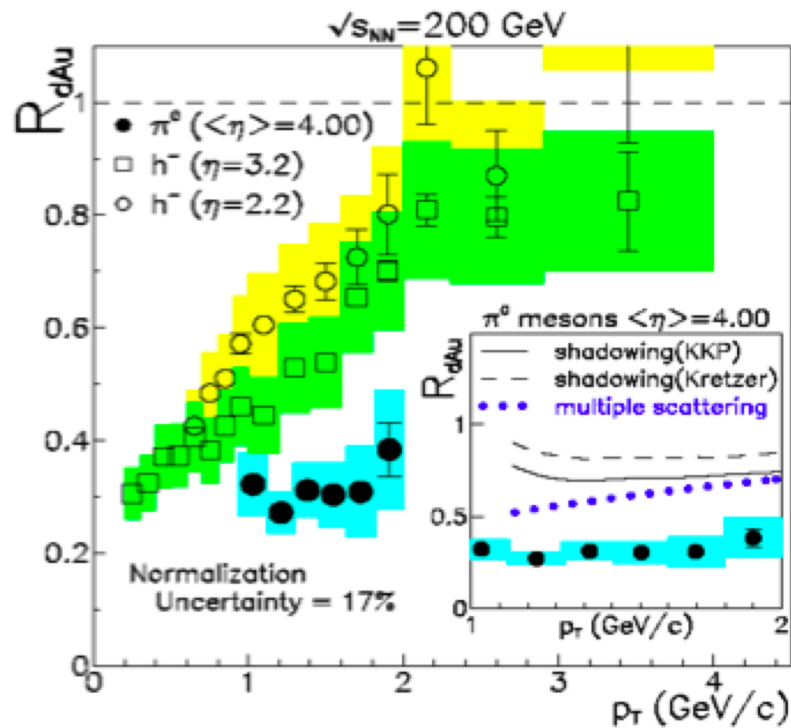
$$R_{dAu} = \frac{1}{2 * 197} \frac{\sigma_{dAu}}{\sigma_{pp}}$$



D. Kharzeev
hep-ph/0307037
As η grows

CGC expects suppression of forward hadron production

Suppression: R_{dAu}



Note that overall π production is suppressed below 3 GeV in dAu compared to pp

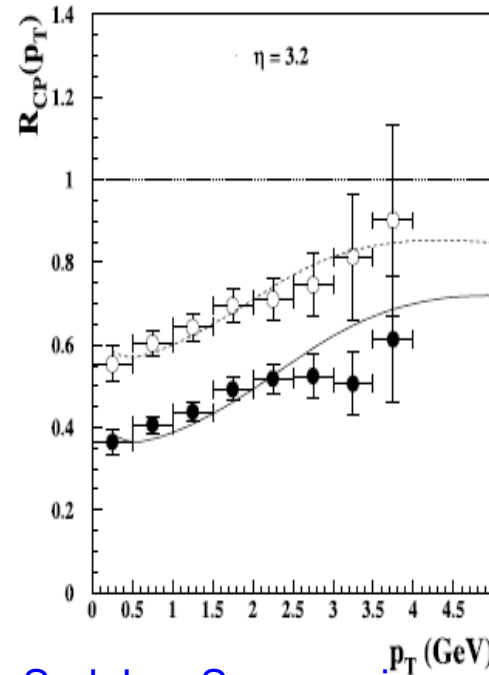
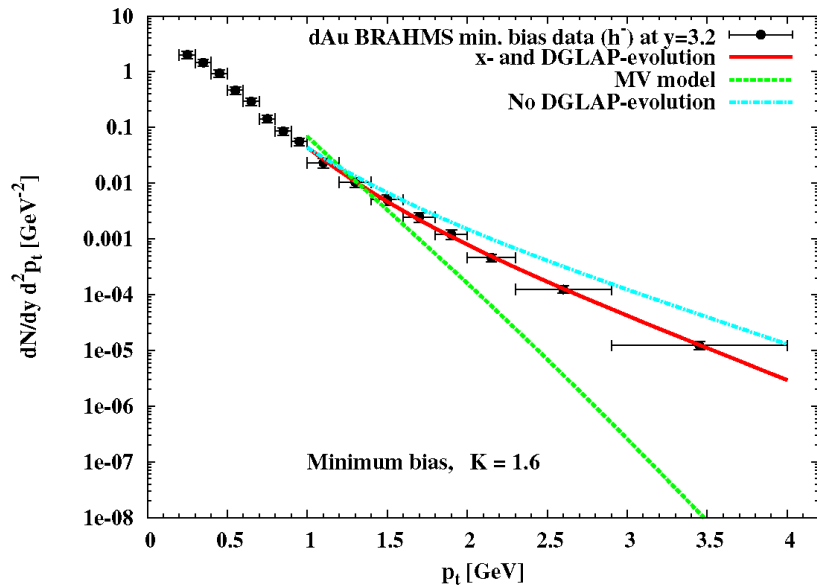
Is saturation really the explanation?

$\eta = 3.2$

Dumitru, Hayashigaki Jalilian-Marian
NP A765, 464



PRL 93, 242303

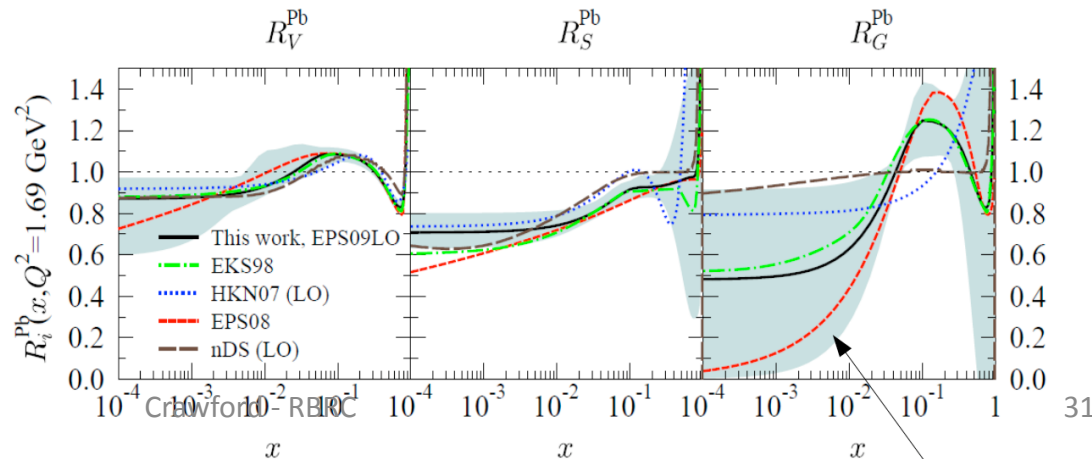


B.Kopeliovich
et. al.
PRC72 054606

A CGC calc. gives a very good description
of the p_T dependence

Sudakov Suppression, not low-x phenomena
Reproduce p_T trend and centrality dependence.

Paukkunen et al (QM09)
EPS09

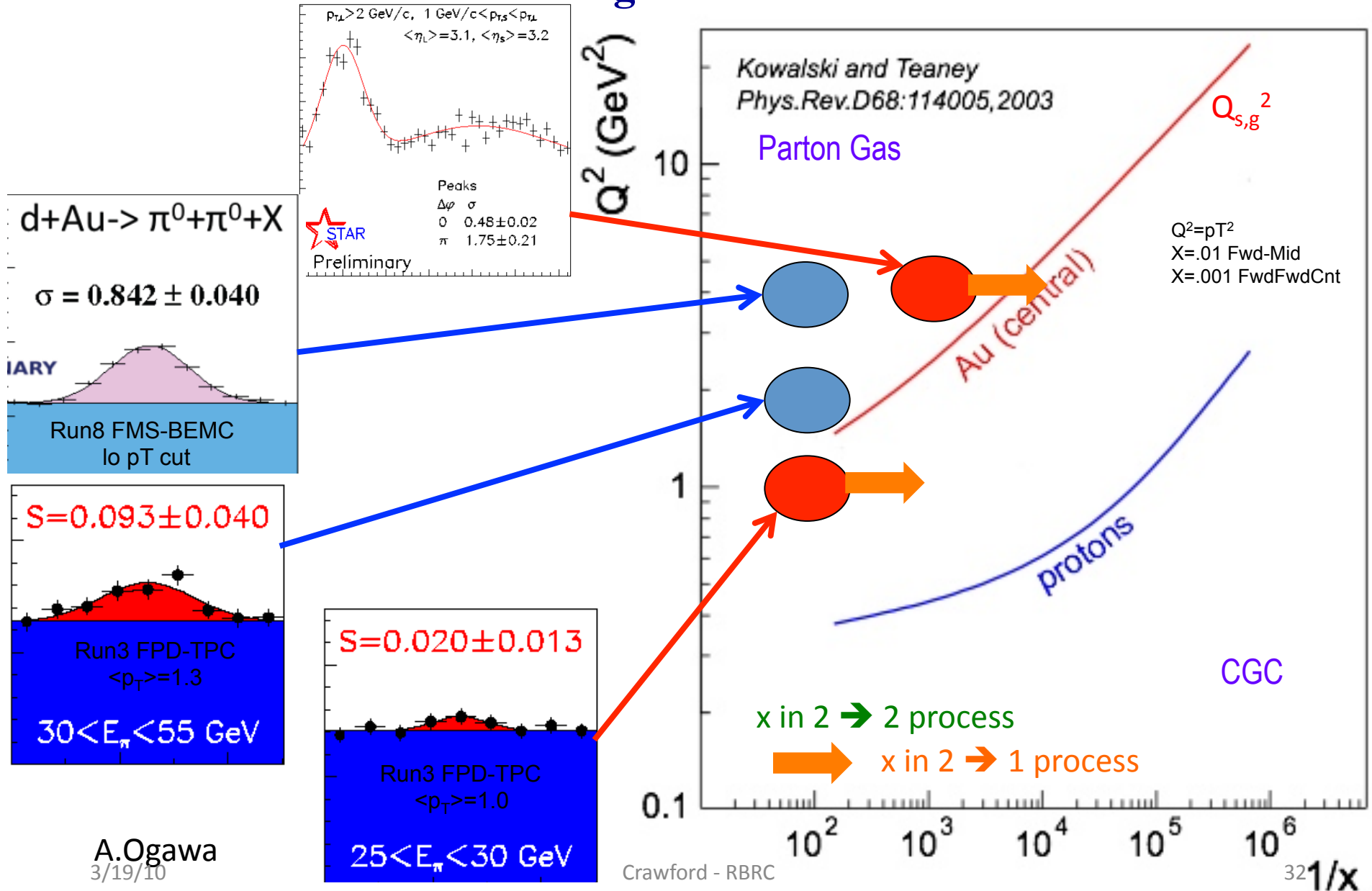


A.Ogawa

5/19/09

Mapping Saturation Scales

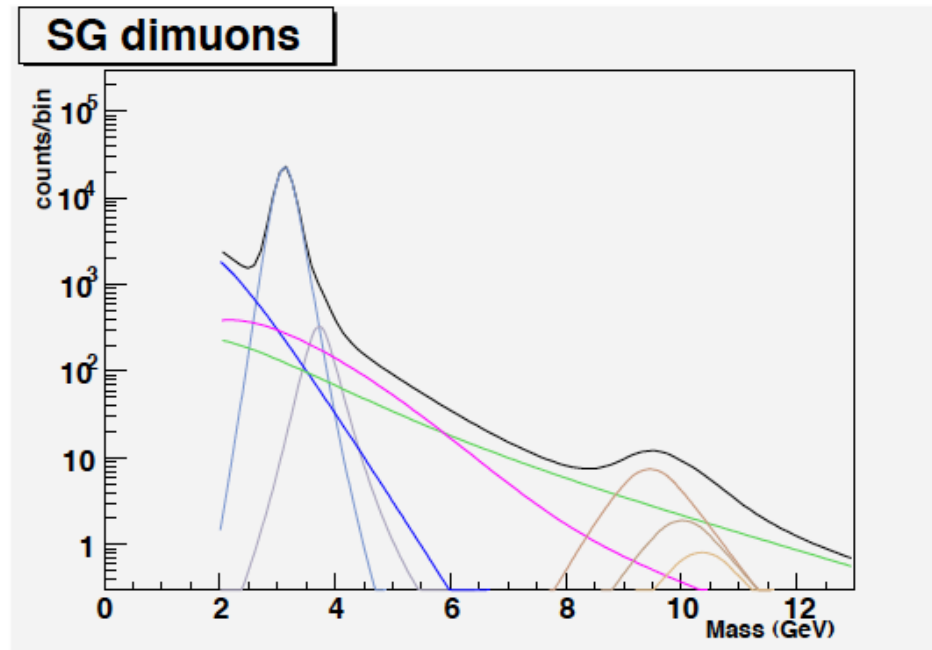
need to get to lower x



DY for lower x

- Drell-Yan $q\bar{q} \rightarrow \gamma^* \rightarrow e^+e^-$ OR $\mu^+\mu^-$
 - $x_F = x_1 - x_2$
 - $M^2 = x_1 \cdot x_2 \cdot s$ where $s = (E_{CM})^2$
 - $x_2 = -x_F \pm \sqrt{x_F^2 + 4M^2/s}$
 - $x_2 = M^2/x_F/s$
 - 250 GeV p on 100 GeV Au
 - For 250 GeV p on 100 GeV Au, get
 - $S^2 = E^2 - p^2 = (250+100)^2 - (250-100)^2 \approx 316 \text{ GeV}$
 - For $M(\gamma^*) = 3.2$
 - $\Rightarrow x_2 = 10^{-4}$
 - Lower $M^* \Rightarrow$ lower x_2

DY M* range



Above J/ψ the
Primary bkgd
Is Υ

Figure 7: Dimuon invariant mass $dN^{\mu^+\mu^-}/dM$ cocktail distributions in the PHENIX muon spectrometer acceptance, from full PYTHIA plus PHENIX detector simulations. Black = Total, Light-Blue = J/Ψ , Light-Gray = Ψ' , Blue = $c\bar{c}$, Magenta = $b\bar{b}$, Green = Drell-Yan, Light-Brown = three Upsilon states.

Forward $J/\psi \rightarrow e^+e^- \rightarrow M(J/\psi)$ measured in FMS at STAR

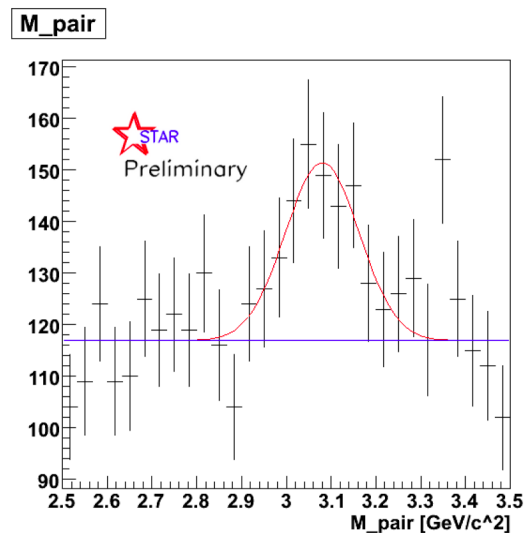


Fig. 8 Reconstructed mass from pairs of clusters observed at forward rapidity with the FMS. Each cluster is subjected to an isolation cut, to reduce backgrounds from neutral pion decay and jet production. A further requirement is imposed on the transverse momentum of the cluster. The Gaussian peak is consistent with observation of J/ψ produced with $\langle x_F \rangle = 0.67$. The x_F dependence of J/ψ production in p+p collisions could come from large-x intrinsic heavy components in the proton wavefunction [12].

DY A_N motivator

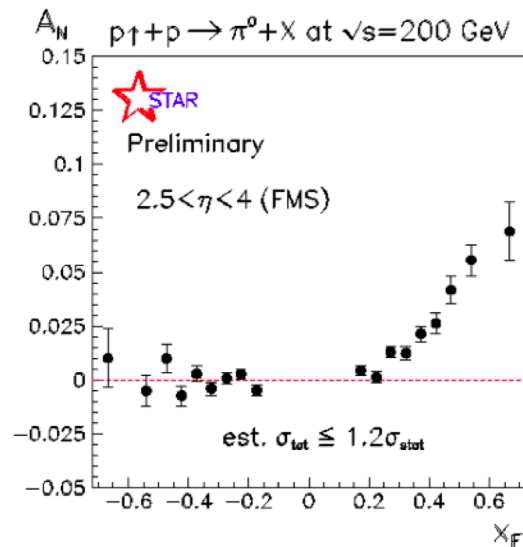
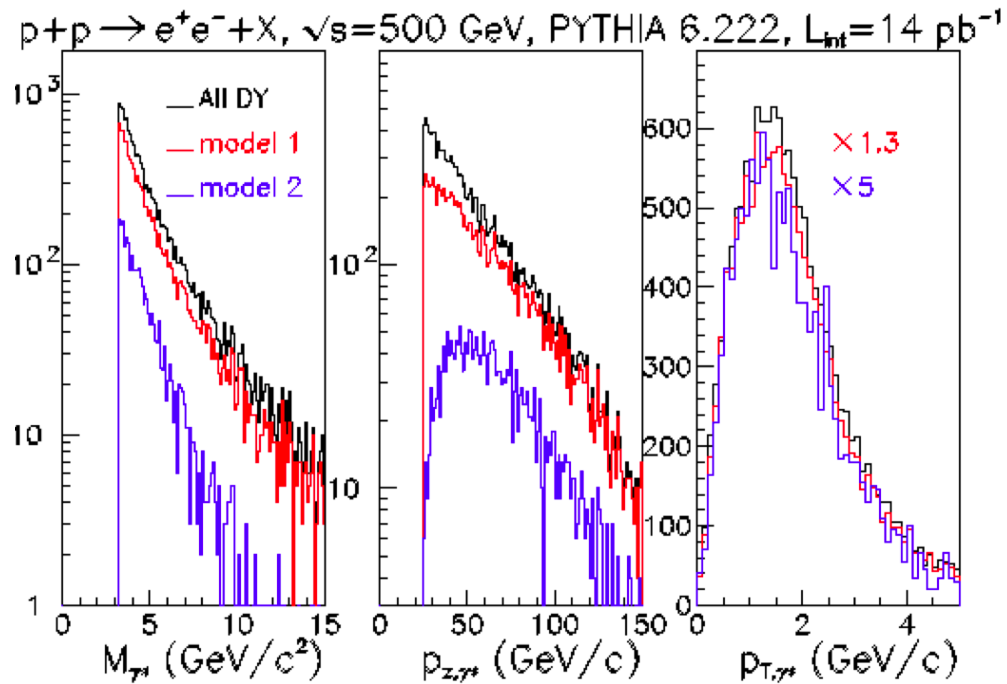


Fig. 5b Feynman x dependence of the analyzing power for π^0 production from the FMS. These results integrate over a different pseudorapidity range from published results [4].

qg interaction leaves different Color field than qqbar leaves.

Apparently more robust calculations concerning color interaction are possible with DY measurements; Color-induced phase differences suggest that $A_N(\text{DY})$ is of different sign than $A_N(\pi^0)$

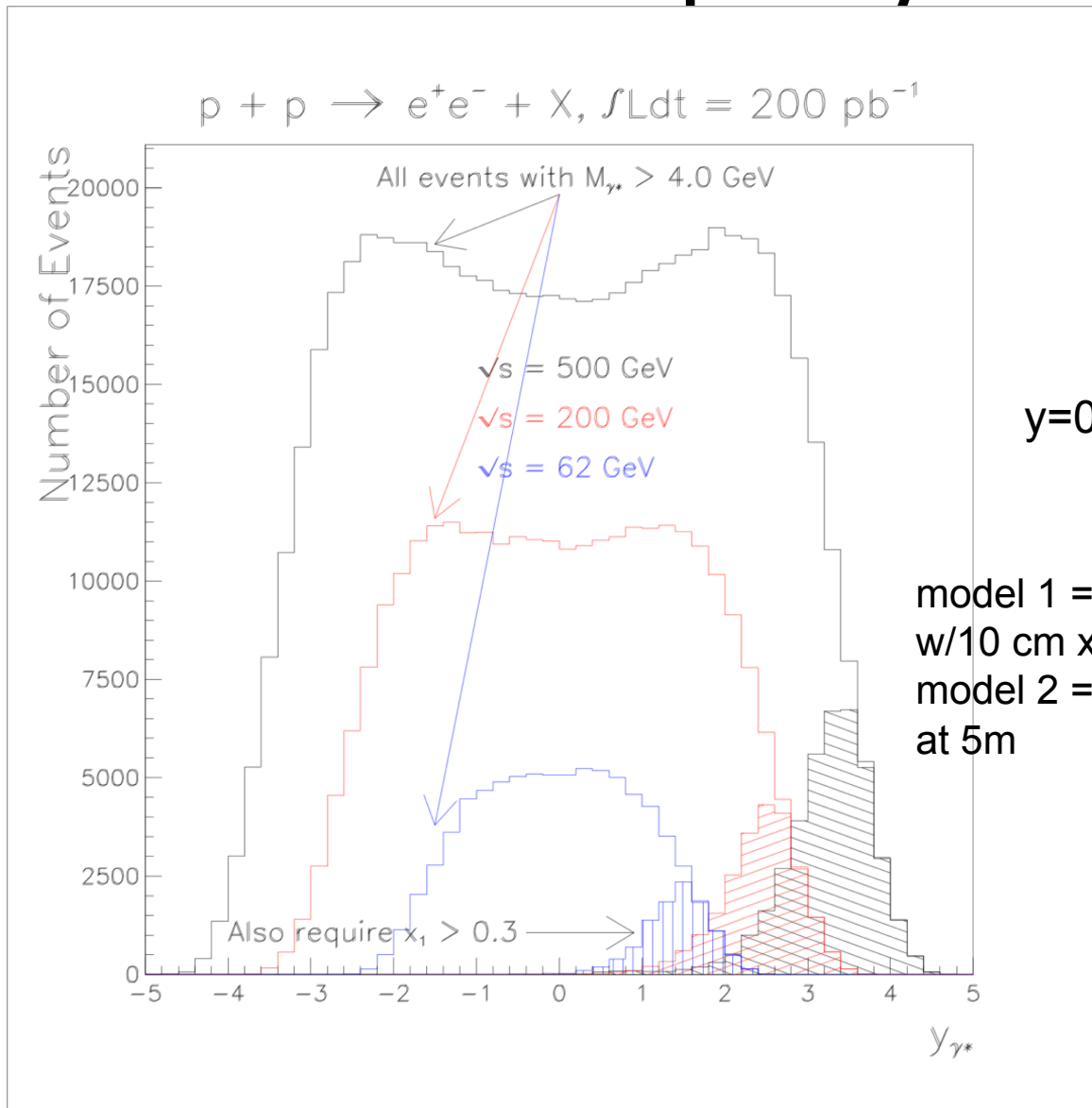
DY spectrum



model 1 = 2x2 m 2 EM+H at 10m
w/10 cm x 10 cm hole
model 2 = existing FHC + EM
at 5m

Fig. 5 Kinematic distributions for the virtual photon. Model 1 would be a final facility and model 2 is the first stage of the proposed feasibility test for studying DY production at RHIC.

DY Yield vs rapidity



$$y = 0.5 \cdot \ln\left(\frac{E + p_z}{E - p_z}\right)$$

model 1 = 2x2 m² EM+H at 10m
w/10 cm x 10 cm hole
model 2 = existing FHC + EM
at 5m

L.Bland

DY test plan

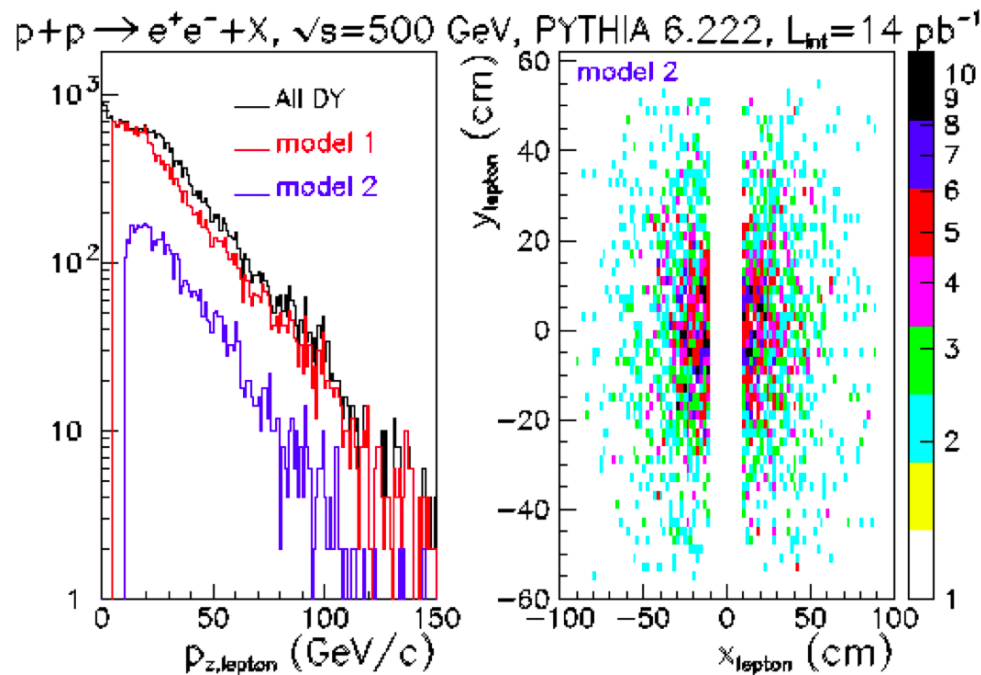


Fig. 10 Kinematic distributions for the electron and positron decay products of the virtual photon. Model 1 would be a final facility and model 2 is the first stage of the proposed feasibility test for studying DY production at RHIC.

DY plan

First – calorimetry (E + H) with charged/neutral selection
we have already seen the J/ψ this way
and that was without any hadron calorimeter

Add tracking if needed

Use all fast detectors and electronics – run at 10 MHz

Determine sign of A_N and requirements for
DY study of x distribution

Outlook

Complete efficiency studies and publish $\pi^0 h$ and $\pi^0 \pi^0$ correlation results for pp and dAu

Complete FMS-EEMC correlations to fill $1 < \eta_2 < 2$ in study of rapidity dependence

Complete J/ψ measurements

Measure $A_N(DY)$ above J/ψ to see color force

Measure $P(x)$ at $x \sim 10^{-4}$ for $M(\gamma^*) > 3.2$ GeV

backup